People's Democratic Republic of Algeria
Ministry of Higher Education and Scientific Research

University M'Hamed BOUGARA – Boumerdes

Institute of Electrical and Electronic Engineering

Department of Power and Control

Final Year Project Report Presented in Partial Fulfilment of the Requirements for the Degree of

MASTER

In **Power Engineering**

Option: **Power Engineering**

Title:

Electrical Parameters Evaluation of a 600W Photovoltaic System installed in the IGEE-Boumerdes University

Presented by:

- **MAZIGHI Brahim**
- **AOUBID Ibrahim**

Supervisor:

DR.R.MEDJOUDJ

Registration Number:……/2019

Abstract

The aim of this project is an evaluation of the electrical parameters of a 600W photovoltaic system; the system consists of four PV modules installed in the yard of the Institute of Electrical and Electronics Engineering (Boumerdes) at a fixed altitude angle of 45º. The MPPT charge controller manages the power flow from the PV modules and batteries to the inverter which supplies a small load. The values of current and voltage at the PV modules and battery stages are taken every five minutes from the morning to the evening, then the results are analyzed using Weibull++ Software to define the parameters of distribution that the data is following, then conclude the mean values of power. The power data are divided into intervals, then the probability of each interval is calculated. The resulting probabilities is used to predict the power generated by the system through that day.

Keywords: Photovoltaic system, PV modules, MPPT charge controller, inverter, Weibull.

DEDICATION

I dedicate this piece of work

To my dear Father, my beloved Mother

To my Brothers and Sisters,

To all my friends

Brahim,

Ibrahim.

Acknowledgments

We are thankful to Allah, the most gracious and the most merciful for helping us finish this modest work.

We would like to express the deepest appreciation to our supervisor **Dr. Rafik MADJOUDJ** for his support and guidance through this project. It has been a privilege to work under his supervision.

Moreover, we would like to thank **Prof. AISSA KHALDOUN** for helping us finishing this work.

Also, we thank the members of the jury for taking the time to read and analyze this thesis, and the teachers of IGEE for the knowledge they passed to us.

No acknowledgement would be complete without expressing our appreciation and thankfulness to our beloved friends especially **Oussama ADDA BENKOCEIR** and **Ismail RAHMANIA** for their help and support.

Last but not least, a big thank you to our families who were there for us since the beginning and for the support and encouragement they have shown us throughout our lives, particularly the last five years.

Table of contents

General Introduction

Chapter One: General Overview on PV System and Weibull ++

Chapter Two: System Hardware components

Chapter Three: Implementation and Measurement Results

Chapter Four: Data analysis using Weibull++

General Conclusion

List of Figures

List of Tables

Abbreviations

AC: Alternative Current.

DC: Direct Current.

V_{oc}: Open Circuit Voltage.

I_{sc}: Short Circuit Current.

FF: Fill Factor.

PV: Photovoltaic.

T_{cell} : Cell Temperature.

T_{amb}: Ambient Temperature.

P_{max}: Maximum Power at STC.

$NOCT$: Nominal Operating Cell Temperature.

MPP: Maximum Power Point.

MPPT: Maximum Power Point Tracking.

AM: Air Mass.

STC: Standard Test Conditions.

SPWM: Sinusoidal Pulse Width Modulation.

SV: Space-Vector.

SHE: Selective-Harmonic-Elimination.

GENERAL INTRODUCTON

GENERAL INTRODUCTION

Due to environmental pollution and global warming effects, renewable energies are considered as the best alternative to fossil energy to avoid these problems. Solar energy is the most important since it is available anywhere and at least 10 hours per day; the sun can provide enough energy to our planet.

Since the beginning of time, people have been fascinated by Sun. Throughout history, they tried to benefit from it and recently scientists have found how to convert this solar energy into an electrical one by using different techniques. Solar energy can be concentrated and used in order to heat water; the vapor of this water drives a turbine. This is called indirect conversion. The direct conversion is done by using photovoltaic technology.

Photovoltaic cells are the basic elements that convert this solar energy; they are made out of semiconductor materials. Photovoltaic modules are a combination of these cells and the combination of these modules gives us photovoltaic arrays. The arrays connected to loads, together are called a Photovoltaic system. They can be on grid-connected or off grid-connected.

A photovoltaic power system can be used to provide alternative and inexhaustible source of electrical power to our homes through the direct conversion of solar irradiance into electricity. The process of acquiring a photovoltaic power system involves designing, selecting and determining the specifications of the different components employed in the system. The success of this process depends on a variety of factors such as geographical location, weather condition, solar irradiance, and load profile.

The purpose of this project is to evaluate the electrical parameters of a real system of 600W installed in the IGEE -Boumerdes. The report is structured into four chapters.

Firstly, chapter one details a general overview of the PV system and Weibull ++ software. The second chapter illustrates the components utilized in the implementation of the system installed and the components of measurement. The third chapter shows the implementation of the system and analyzes its results. Finally, the fourth chapter defines the distribution of

data and its behavior, then determines the electrical parameters and the mean values of energy production that are estimated. Weibull++ software is used to carry out this study.

Chapter One

GENERAL OVERVIEW ON PV SYSTEM AND WEIBULL++

1.1 Introduction

In this chapter, a general overview about solar cells, their principal of operation and the effects of temperature and irradiance on them will be given. Also, the Weibull distribution and its characteristics will be discussed.

1.2 History of solar cells

Solar cell's early days go back to 1839, Edmund Becquerel, a French physicist, discovered the solar cell effect while experimenting with an electrolytic cell made up of two metal electrodes. From that day, scientists and researchers kept developing the photovoltaic cell technology, yielding many of the following discoveries: [1]

- 1873–1876: Selenium's Photoconductivity is discovered by English electrical engineer Willoughby Smith.
- In 1883, New York inventor Charles Fritts created the first solar cell by coating selenium with a thin layer of gold.
- In 1887, German physicist Heinrich Hertz first observed the photoelectric effect.
- 1953–1956: Silicon Solar Cells are produced commercially.
- Thomas Faludy filed a patent in 1995 for a retractable awning with integrated solar cells.
- In 1994, the National Renewable Energy Laboratory developed a new solar cell from gallium indium phosphide and gallium arsenide that exceeded 30% conversion efficiency.
- 2005: DIY Solar Panels Became Popular.[1]

1.3 Working principle of solar cells

The working principle of all today's solar cells is essentially the same. It is based on the photovoltaic effect. In general, the photovoltaic effect means the generation of a potential difference at the junction of two different materials in response to visible or other radiations. Most cells are made of a layer of silicon, which is a semiconductor. A layer of phosphorus is added at the top and a layer of boron at the bottom. The whole is placed between two glass plates for protection. As soon as sunlight shines on a solar cell, electrons are detached from the top of the cell under the influence of this radiation; there is a free electron and its

corresponding hole. Because an electric field arises at the interface due to the uneven charge distribution, the electrons can only go one way. As a result, a voltage difference between the top and bottom of the cell occurs. If you connect the top and bottom, a current will flow across the wire. Since the voltage across the cell is very low (only 0.5V), several cells are often knotted together in a module. [2] As the following Figure illustrates:

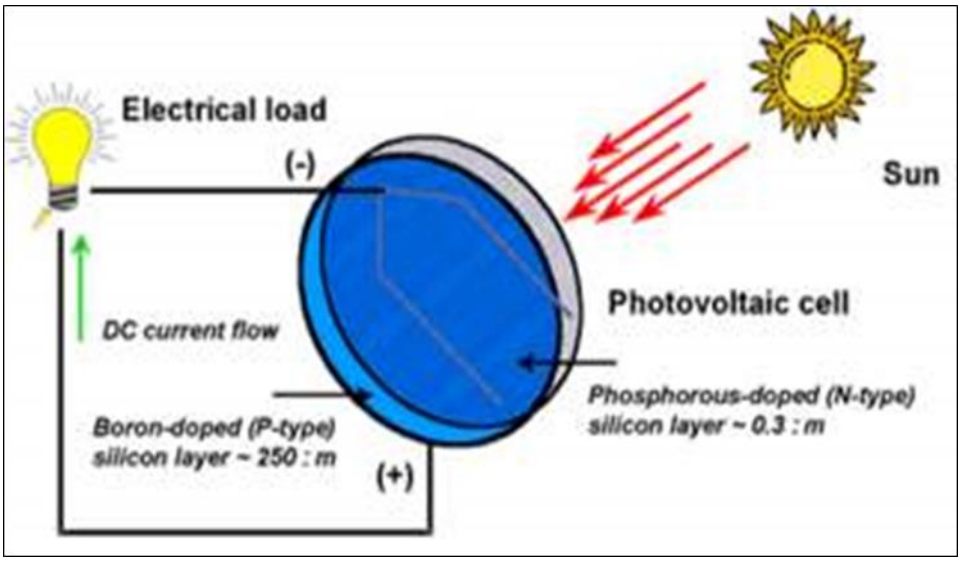

Figure 1.1: Schematic of the working principal of the solar cell. [2]

1.4 Solar cell equivalent circuit and characteristic equation

The equivalent circuit of a solar cell is shown below:

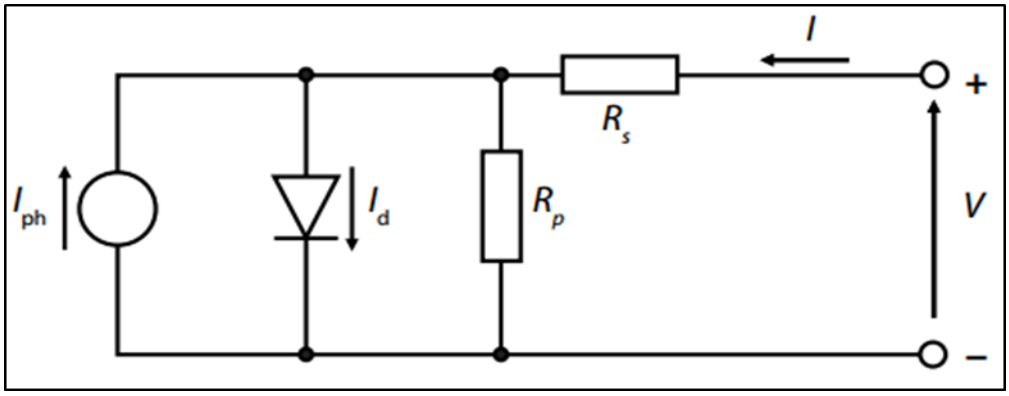

Figure 1.2: The equivalent circuit of a solar cell.

The characteristic equation of a solar cell, which relates solar cell parameters to the output current and voltage is given by:

$$I = I_L - I_0 \left\{ \exp\left[\frac{q(V+IR_s)}{nKT}\right] - 1 \right\} - \frac{V+IR_s}{R_{SH}} \quad (1.1)$$

where:

- I: output current (A).
- I_0: reverse saturation current (A).
- V: voltage across the output terminals (V).
- n: diode ideality factor (1 for an ideal diode).
- q: elementary charge.
- K: Boltzmann's constant value.
- T: absolute temperature at 25°C.
- R_{SH}: shunt resistance (Ω).
- R_s: series resistance (Ω).[3]

1.5 Photovoltaic Generator

A solar cell is the most basic element in a photovoltaic system. Cells are too small to do much work. They only produce about 0.5 V, and usually the system requires 12V or more to charge batteries or run motors. A typical module is a group of PV cells connected in series and encapsulated. The key purpose of encapsulating a set of electrically connected solar cells, is to protect them and their interconnecting wires from the typically harsh environment in which they are used. Usually commercial modules consist of 36 or 72 cells. For high voltage requirements, modules are connected in series; but for high current requirements, they are connected in parallel. High power requirements need connections in series and in parallel. Such a combination of modules is called a PV array (see figure1.3). [4]

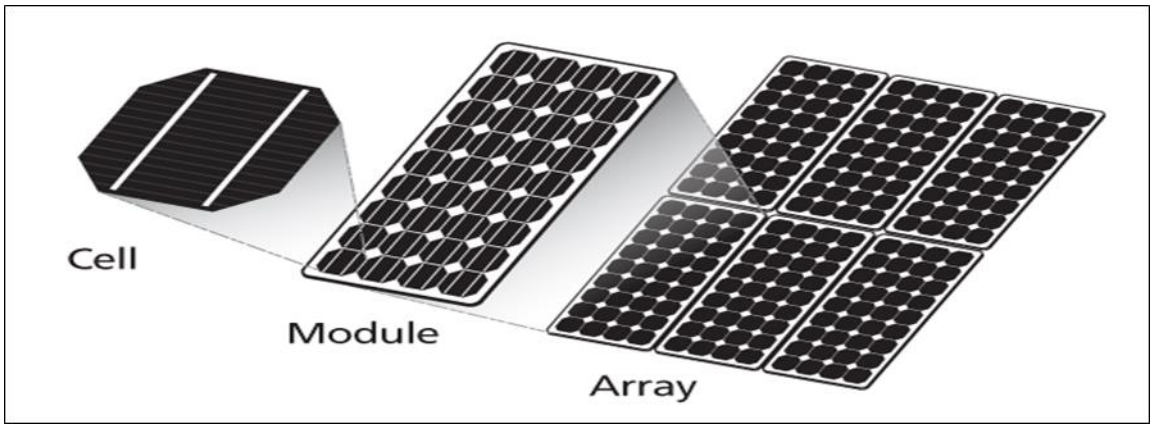

Figure 1.3: The photovoltaic generators.

1.6 Solar Cell parameters

The main parameters that are used to characterize the performance of solar cells are the peak power P_{MAX}, the short-circuit current I_{SC}, the open circuit voltage V_{OC} and the fill factor FF. The cell voltage, current and power at the maximum power point are V_{MPP}, I_{MPP}, and, P_{MPP}, respectively. [5]

1.6.1 Short Circuit current (I_{sc})

The short-circuit current Isc is the current that flows through the external circuit when the electrodes of the solar cell are short circuited. It is the maximum possible current in the circuit. [5] The equation of the short circuit current is directly proportional to the available sunlight:

$$I_{SC} = qg(L_n + L_p) = I_L \quad (1.2)$$

Where:

- I_L: light generated current (A).
- g: the generation rate.
- Ln: the electron diffusion lengths (cm).
- Lp: the hole diffusion lengths (cm).
- q: elementary charge (C).

1.6.2 Open Circuit voltage (V_{OC})

The open-circuit voltage is the voltage at which no current flows through the external circuit. It is the maximum voltage. In other words, open circuit voltage represents the maximum possible voltage value, which occurs when a high impedance load is connected to the circuit or in the case of no-load.[5]

$$V_{oc} = \frac{kT}{q} \ln\left(\frac{I_L}{I_o} + 1\right) \quad = \frac{kT}{q} \ln\left(\frac{I_L}{I_o}\right) \tag{1.3}$$

Where:

- Io: Dark saturation current.
- k: Boltzmann's constant.
- T: Temperature in Kelvin (Tc°+273).

1.6.3 Maximum Power Point (MPP)

In the case of a short circuit or an open circuit operating point, no power is generated. As a result, the operating point should fall into the range of the maximum power output of the PV cell. This operating point is determined by choosing the correct value of the connected load.[5]

The maximum power output is defined as the product of the voltage and the current at the MPP:

$$P_{max} = V_{MPP} \times I_{MPP} \tag{1.4}$$

Where V_{MPP} and I_{MPP} are voltage and current values that give the maximum operating power.

1.6.4 Fill Factor (FF)

The fill factor (FF) is an indicator of the quality of the PV cell. It is the ratio between the maximum power (Pmax = Impp*Vmpp) generated by a solar cell and the product of Voc with Isc. The maximum value of the fill factor is theoretically unity. The maximum practical value in silicon is 0.88.[5]

$$FF = \frac{P_{max.\,practical}}{Pmax.theorotical} = \frac{V_{mp} \times I_{mp}}{V_{oc} \times I_{sc}} \quad (1.5)$$

For a good I-V curve profile with fill factor close to unity, the current should stay constant while the voltage increases till the operating point reach the knee of the curve. After that point, the current of PV cell should gradually decrease.

1.6.5 Efficiency of solar cells

Efficiency is defined as the ratio of energy output from the solar cell to input energy from the sun. In addition to reflecting the performance of the solar cell itself, the efficiency depends on the spectrum and intensity of the incident sunlight and the temperature of the solar cell. Therefore, conditions under which efficiency is measured must be carefully controlled in order to compare the performance of one device to another. Terrestrial solar cells are measured under AM1.5 conditions and at a temperature of 25°C. Solar cells intended for space use are measured under AM0 conditions.[6] The efficiency of a solar cell is determined as the fraction of incident power which is converted to electricity and is defined as:

$$P_{max} = V_{oc} I_{sc} FF \quad (1.6) \quad ; \quad \eta = \frac{V_{oc} I_{sc} FF}{P_{in}} \quad (1.7)$$

Where:

- V_{oc}: the open-circuit voltage.
- I_{sc}: the short-circuit current.
- FF: the fill factor and η is the efficiency.

The input power for efficiency calculations is 1 kW/m^2 or 100 mW/cm^2. Thus, the input power for a 100 × 100 mm^2 cell is 10 W and for a 156 × 156 mm^2 cell is 24.3 W.

1.7 I-V and P-V curves of a PV device

A current-voltage (I-V) curve shows the possible combinations of the current and voltage output of a photovoltaic (PV) device. The I-V curve is based on the device being under Standard Test Conditions (1 kW/m2, AM 1.5, 25°C Cell Temperature). The main points of the I-V curve characteristics are the short-circuit current (Isc), the open-circuit voltage (Voc)

and there is a point on the knee of the curve where the maximum power output is located. the power-voltage (P-V) curve is the product of the current and voltage for each point in the I-V curve. This product represents the output power for that operating condition. The MPP produced by the PV generator is reached at a point on the characteristic where the product I-V is maximum (see Figure1.4). [7]

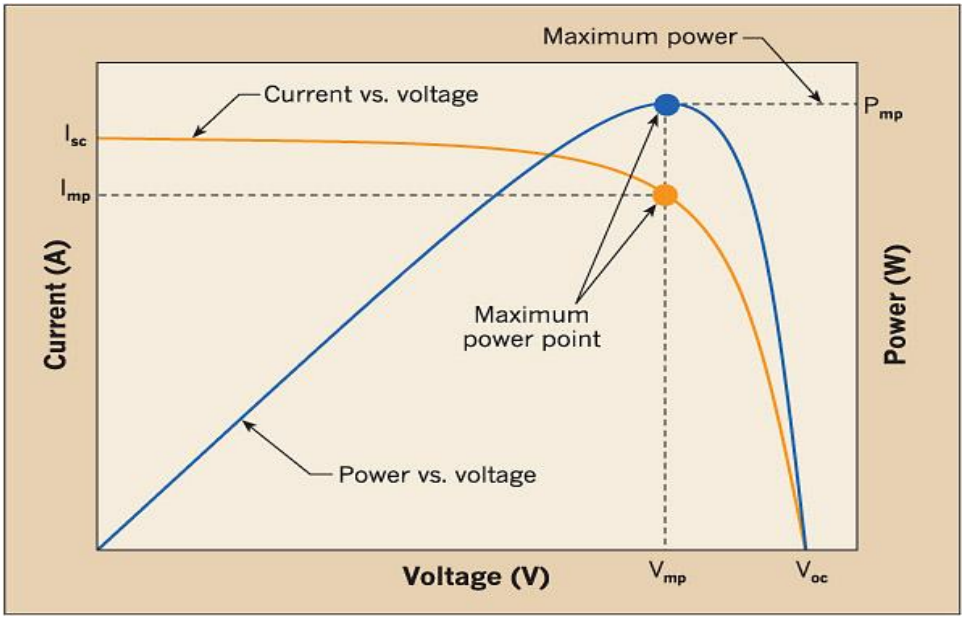

Figure 1.4: I-V and P-V curves of a PV device.[7]

1.8 Temperature effects

Solar cells are sensitive to temperature like all other semiconductor devices. Increases in temperature reduce the band gap of a semiconductor, thereby affecting most of the semiconductor material parameters. The decrease in the band gap of a semiconductor with increasing temperature can be viewed as increasing the energy of the electrons in the material. Lower energy is therefore required to break the bond. In the bond model of a semiconductor band gap, reduction in the bond energy also reduces the band gap. Therefore, increasing the temperature reduces the band gap. [8]

In a solar cell, the parameter most affected by an increase in temperature is the open-circuit voltage and this change affects the power too. The impact of increasing temperature is shown in the figure below:

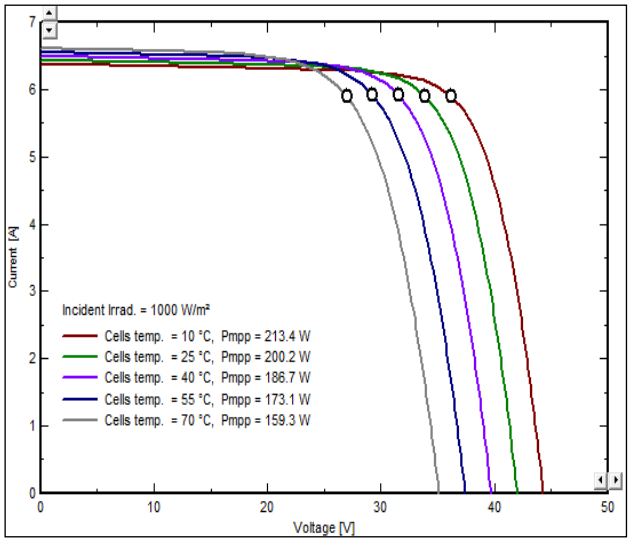

Figure 1.5 (a): The effect of temperature on the PV module's voltage.

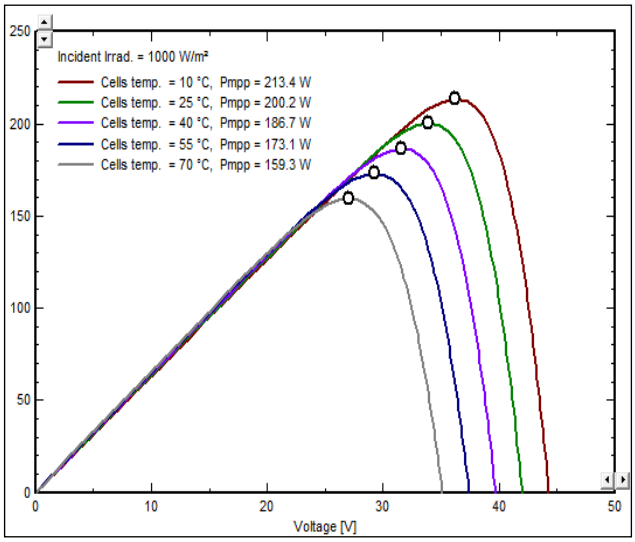

Figure1.5 (b): The effect of temperature on the PV module's power.

The open-circuit voltage decreases with temperature because of the temperature dependence of I_0. The equation for I_0 from one side of a p-n junction is given by:

$$I_0 = qA\frac{Dn_i^2}{LN_D} \tag{1.9}$$

Where:

- q: the electron charge.
- A: the area.
- D: the diffusivity of the minority carrier.
- L: the minority carrier diffusion length.
- N_D: the doping concentration.
- n_i: the intrinsic carrier concentration.

In the above equation, many of the parameters have some temperature dependence, but the most significant effect is due to the intrinsic carrier concentration(n_i). The intrinsic carrier concentration depends on the band gap energy (with lower band gaps giving a higher intrinsic carrier concentration), and on the energy which the carriers have (with higher

temperatures giving higher intrinsic carrier concentrations). The equation for the intrinsic carrier concentration is: [8]

$$n_i^2 = 4\left(\frac{2\pi KT}{h^2}\right)^3 (m_e^* m_h^*)^{3/2} \exp\left(-\frac{E_{G0}}{KT}\right) = BT^3 \exp\left(-\frac{E_{G0}}{KT}\right) \quad (1.10)$$

Where:

- T: the temperature.
- h and k are constants.
- me and mh are the effective masses of electrons and holes respectively.
- EGO: the band gap linearly extrapolated to absolute zero temperature.
- B: a constant which is essentially independent of temperature.

The following expression is used to calculate the cell temperature:

$$T_{cell} = T_{amb} + \left(\frac{NOCT - 20}{0.8}\right).G \quad (1.11)$$

Where:

- T_{cell} : cell temperature (°C).
- T_{amb}: ambient temperature.
- G: solar insolation (kW/m2).

Substituting these equations back into the expression for I_0 and assuming that the temperature dependencies of the other parameters can be neglected, gives:

$$I_0 = qA\frac{D}{LN_D} BT^3 \exp\left(-\frac{E_{G0}}{KT}\right) \approx B'T^{\gamma} \exp\left(-\frac{E_{G0}}{KT}\right) \quad (1.12)$$

where

- B': a temperature independent constant.
- A: a constant value.
- Γ: used instead of the number 3 to incorporate the possible temperature dependencies of the other material parameters.

For silicon solar cells near room temperature, I_0 approximately doubles for every 10 °C increase in temperature. [8]

The impact of I_0 on the open-circuit voltage can be calculated by substituting the equation for I_0 into the equation for V_{oc} as shown below:

$$V_{oc} = \frac{KT}{q} ln\left(\frac{I_{sc}}{I_0}\right) = \frac{KT}{q} lnI_{sc} - \frac{KT}{q} ln\left[B'T^{\gamma} exp\left(-\frac{qV_{G0}}{KT}\right)\right]$$

$$V_{oc} = \frac{KT}{q}\left(lnI_{sc} - lnB' - \gamma lnT + \frac{qV_{G0}}{KT}\right) \quad (1.13)$$

Where $E_{G0} = qV_{G0}$.

Assuming that dVoc/dT does not depend on dIsc/dT, dVoc/dT can be found as:

$$\frac{dV_{oc}}{dT} = \frac{V_{oc} - V_{G0}}{T} - \gamma \frac{K}{q} \quad (1.14)$$

The above equation shows that the temperature sensitivity of a solar cell depends on its open circuit voltage, with higher voltage solar cells being less affected by temperature. For silicon, EG0 is 1.2, and using γ as 3 gives a reduction in the open-circuit voltage of about 2.2 mV/°C:

$$\frac{\mathrm{dV_{oc}}}{\mathrm{dT}} = -\frac{\mathrm{V_{G0} - V_{oc} + \gamma \frac{KT}{q}}}{\mathrm{T}} \approx -2.2\mathrm{mV\ per℃\ for\ Si} \quad (1.15)$$

The short-circuit current, I_{sc} increases slightly with temperature, since the band gap energy E_G decreases and more photons have enough energy to create e-h pairs. [8]

However, this is a small effect and the temperature dependence of the short-circuit current from a silicon solar cell is:

$$\frac{1}{\mathrm{I_{sc}}}\frac{\mathrm{dI_{sc}}}{\mathrm{dT}} \approx 0.0006\mathrm{mA\ per\ ℃\ for\ Si} \quad (1.16)$$

or 0.06% mA per °C for silicon.

The temperature dependency FF for silicon is approximated by the following equation:

$$\frac{1}{FF}\frac{dFF}{dT} \approx \left(\frac{1}{V_{oc}}\frac{dV_{oc}}{dT} - \frac{1}{T}\right) \approx -0.0015 per\ ℃ for\ Si \quad (1.17)$$

The effect of temperature on the maximum power output, P_m, is:

$$\mathrm{P_{Mvar}} = \frac{1}{\mathrm{P_M}}\frac{\mathrm{dP_M}}{\mathrm{dT}} = \frac{1}{\mathrm{V_{oc}}}\frac{\mathrm{dV_{oc}}}{\mathrm{dT}} + \frac{1}{\mathrm{FF}}\frac{\mathrm{dFF}}{\mathrm{dT}} + \frac{1}{\mathrm{I_{sc}}}\frac{\mathrm{dI_{sc}}}{\mathrm{dT}} \quad (1.18)$$

$$\frac{1}{\mathrm{P}_M}\frac{\mathrm{dP}_M}{\mathrm{dT}} \approx -(0.004\ \mathrm{to}\ 0.005)\mathrm{mW\ per\ ℃\ for\ Si} \quad (1.19)$$

or 0.4% to 0.5% per °C for silicon.

1.9 Effects of the irradiation on the module's Performance

In a solar cell, the parameter most affected by an increase in irradiation is the short-circuit current and this change affects the power too, but has a small effect on the PV module's open circuit voltage. The impact of increasing irradiation is shown in the figures below:

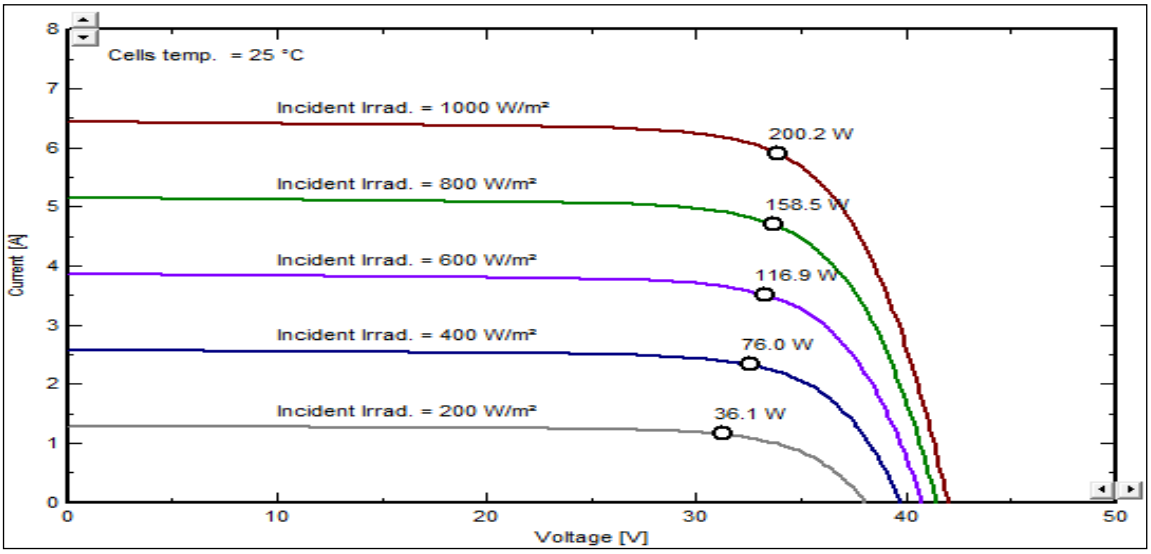

Figure 1.6 (a): Irradiations effect on the PV module's current.

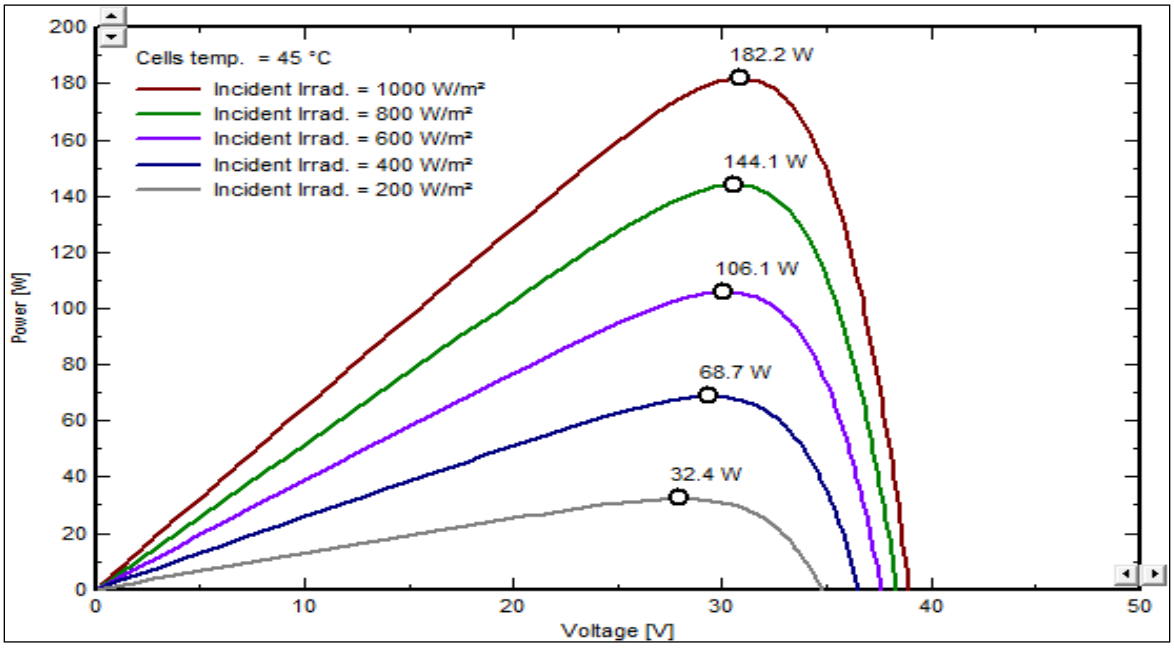

Figure 1.6 (b): Irradiations effect on the PV module's power.

1.10 Overview on Weibull++ Software

1.10.1 Definition

Weibull++ software is the industrial standard in life data analysis (Weibull analysis) for thousands of companies worldwide. Weibull++ provides the most comprehensive toolset available for reliability life data analysis, calculated results, plots and reporting. The software supports all data types and all commonly used product lifetime distributions. The software is also packed with tools related to data analysis, such as warranty data analysis, degradation data analysis, non-parametric data analysis, recurrent event data analysis, reliability test design and experiment design & analysis (DOE). [9]

1.10.2 Weibull distribution

Statistical distributions have been formulated by statisticians, mathematicians and engineers to mathematically model or represent certain behaviors. The Weibull distribution is one of the most widely used lifetime distributions to represent the models. It is a versatile distribution that can take on the characteristics of other types of distributions, based on the value of the shape parameter β as illustrated in figure 1.7. [9]

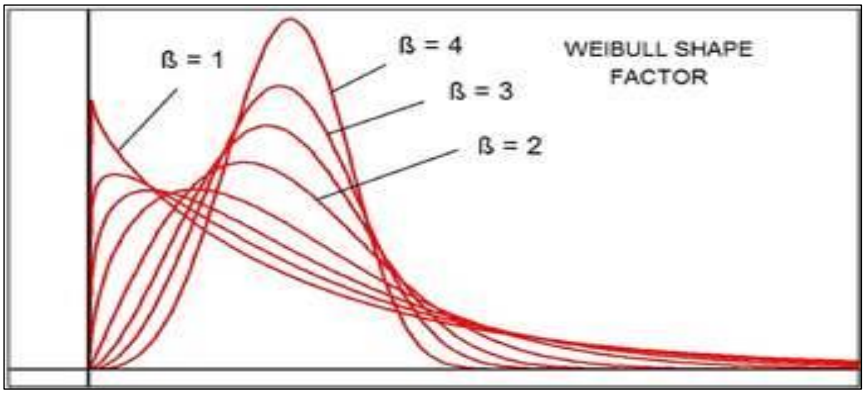

Figure 1.7: The Weibull distribution with different values of β.[10]

The probability density function (pdf) and cumulative density function (cdf) are mathematical functions that describe the distribution. The pdf and cdf of the Weibull distribution are represented mathematically or on a plot where the x-axis represents the variable, and the y-axis represents the function. [9]

The 2-parameter Weibull pdf is given by:

$$f(x) = \frac{\beta}{\eta}\left(\frac{x}{\eta}\right)^{\beta-1} e^{-\left(\frac{x}{\eta}\right)^{\beta}} \quad (1.20)$$

where:

$$f(x) \geq 0 \quad , \quad x \geq 0 \quad , \quad \beta > 0 \quad , \quad \eta > 0$$

and:

- η : the scale parameter, or the characteristic life.
- β : the shape parameter (or slope).

The 2-parameter Weibull cdf is given by:

$$F(x) = 1 - e^{-\left(\frac{x}{\eta}\right)^{\beta}} \quad (1.21)$$

The mean value T of the Weibull pdf is given by:

$$T = \eta.\Gamma\left(\frac{1}{\beta} + 1\right) \quad (1.22)$$

Where $\Gamma\left(\frac{1}{\beta} + 1\right)$ is the gamma function.

$$\Gamma(n) = \int_0^{\infty} e^{-x} x^{n-1}\, dx \quad (1.23)$$

1.10.3 Mixed Weibull distribution

The mixed Weibull distribution (also known as a multimodal Weibull) is used to model data that does not fall on a straight line on a Weibull probability plot. Data of this type, particularly if the data points follow an S-shape on the probability plot, may be indicative of more than one mode at work in the population. Field data from a given mixed population may frequently represent multiple modes, each mode has its subpopulation, the Mixed Weibull Equation is depending on the number of subpopulations chosen.[9] The mixed Weibull cdf is given by:

$$F(x) = \sum_{i=0}^{n} \rho_i \,.\, e^{-\left(\frac{x}{\eta_i}\right)^{\beta}} \quad (1.24)$$

Where ρ is the portion:

$$\sum_{i=1}^{n} \rho_i = 1$$

1.10.4 Confidence bounds

Because life data analysis results are estimates based on the sampling of units, there is uncertainty in the results due to the limited sample sizes. "Confidence bounds" (also called "confidence intervals") are used to quantify this uncertainty due to sampling errors by expressing the confidence that a specific interval contains the quantity of interest. Whether or not a specific interval contains the quantity of interest is unknown.Confidence bounds can be expressed as two-sided or one-sided. Two-sided bounds are used to indicate that the quantity of interest is contained within the bounds with a specific confidence. [9]

1.10.5 Kolmogorov-Smirnov test

In statistics, the Kolmogorov–Smirnov test (K–S test) is a nonparametric test of the equality of continuous or discontinuous samples. One-dimensional probability distributions can be used to compare a sample with a reference probability distribution or to compare two samples. It is named after Andrey Kolmogorov and Nikolai Smirnov.

The Kolmogorov–Smirnov statistic quantifies a distance between the empirical distribution function of the sample and the cumulative distribution function of the reference distribution or between the empirical distribution functions of two samples.

The Kolmogorov–Smirnov test can be modified to serve as a ‘fitness’ test. Weibull++ is a statistical software that supports it.[10]

1.11 Conclusion

This chapter describes the working principal of solar cells, solar cell parameters, the effects of temperature and irradiance on photovoltaic modules. It also describes the Weibull distribution features.

Chapter Two

SYSTEM HARDWARE

COMPONENTS

2.1 Introduction

This chapter delves in the main components of the implementation circuit. The circuit is designed to be used a small stand-alone system which can be extended. It consists of four PV modules, a MPPT charge controller, a single-phase inverter, two batteries and a small load.

2.2 The Photovoltaic modules identification

The ENG36P150W Photovoltaic module is used in the implementation, which is made of 36 poly-crystalline cells connected in series. The table 2-1 presents the characteristics of the solar module under standard test conditions (STC) from the data sheet. The size of each PV module is illustrated in figure 2.1(All lengths are taken in cm.).

Since the maximum voltage from each module is 18.65V, it needs to be increased to exceed 24 volts at the MPPT solar entrance. To do that, each two PV modules are connected in series, then the two strings in parallel as shown in the figure 2.2. The PV modules are installed in the institute yard on a support at a fixed altitude angle of 45º as the figure 2.3 depicts.

Table 2.1: ENG36P150W characteristics under STC.

P_{max}	150W
V_{oc}	23.06
I_{sc}	9.30
V_{mpp}	17.68
I_{mpp}	8.49
$NOCT$	45
$T.C.V_{oc}$[1]	-0.32%
$T.C.I_{sc}$[2]	0.05%
T.C.P_{max}[3]	-0.45%

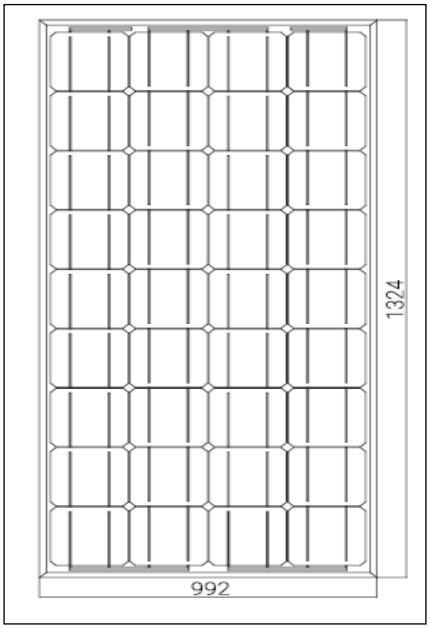

Figure 2.1: Dimensions of the PV Module.

[1] Temperature coefficient of V_{oc} (%/deg.C).
[2] Temperature coefficient of I_{sc} (%/deg.C).
[3] Temperature coefficient of P_{max}(%/deg.C).

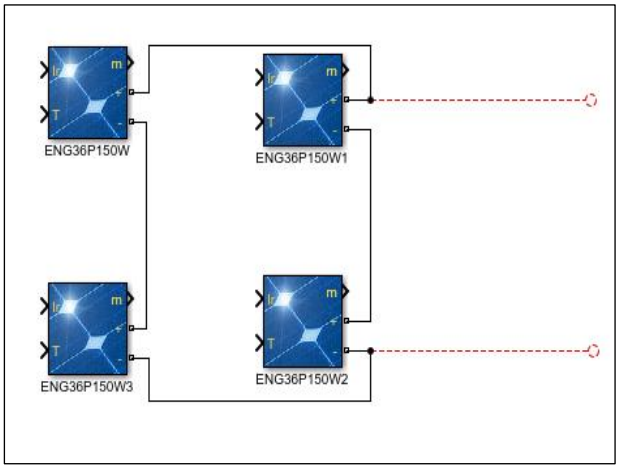

Figure 2.2: The connection of the PV Modules.

Figure 2.3: The PV array site.

After several tests, the datasheet values appear to be inaccurate. An identification test is done to the array to derive more accurate parameters.

2.2.1 Identification test

To conclude the new I-V and P-V curves, two variable resistors of 10.5Ω each, which can support up to 21 A are connected in series to the PV array terminals. Firstly, the value of current and voltage are taken at full resistance, then the resistance is reduced and new values are taken each time. The values of current and voltage for different values of resistance are taken at specific conditions (irradiance is around 1000 w/m and the ambient temperature is 28 ℃).

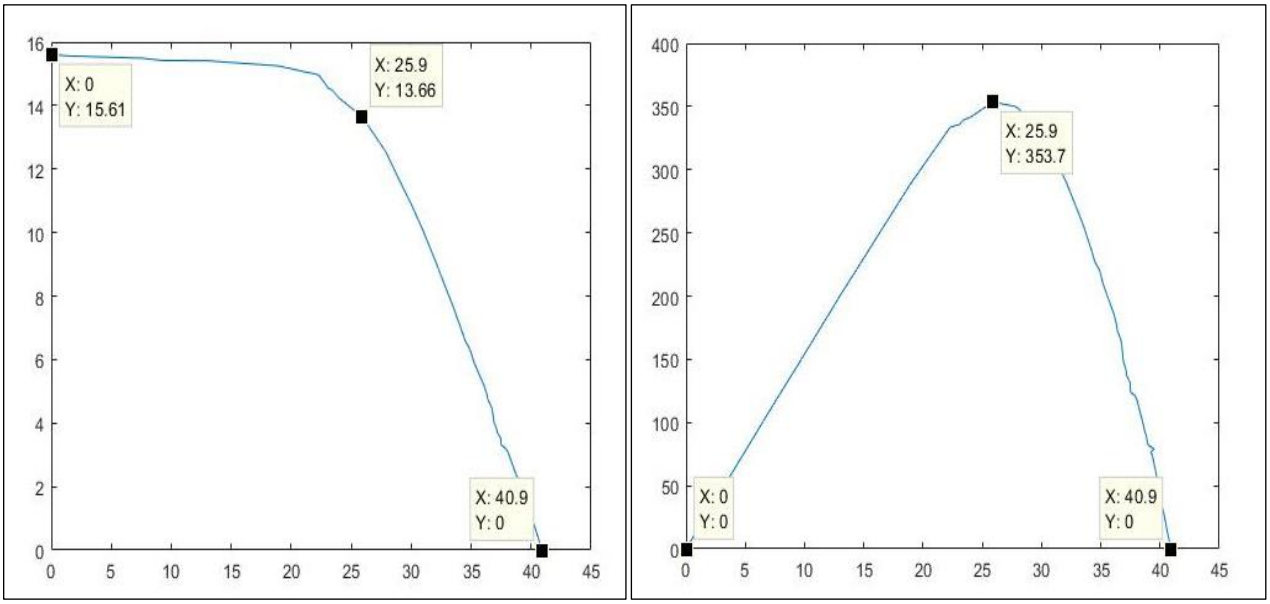

Figure 2.4: I-V and P-V curves for the PV array.

After dividing the voltages and currents over two, the I-V and P-V curves for a single module are plotted:

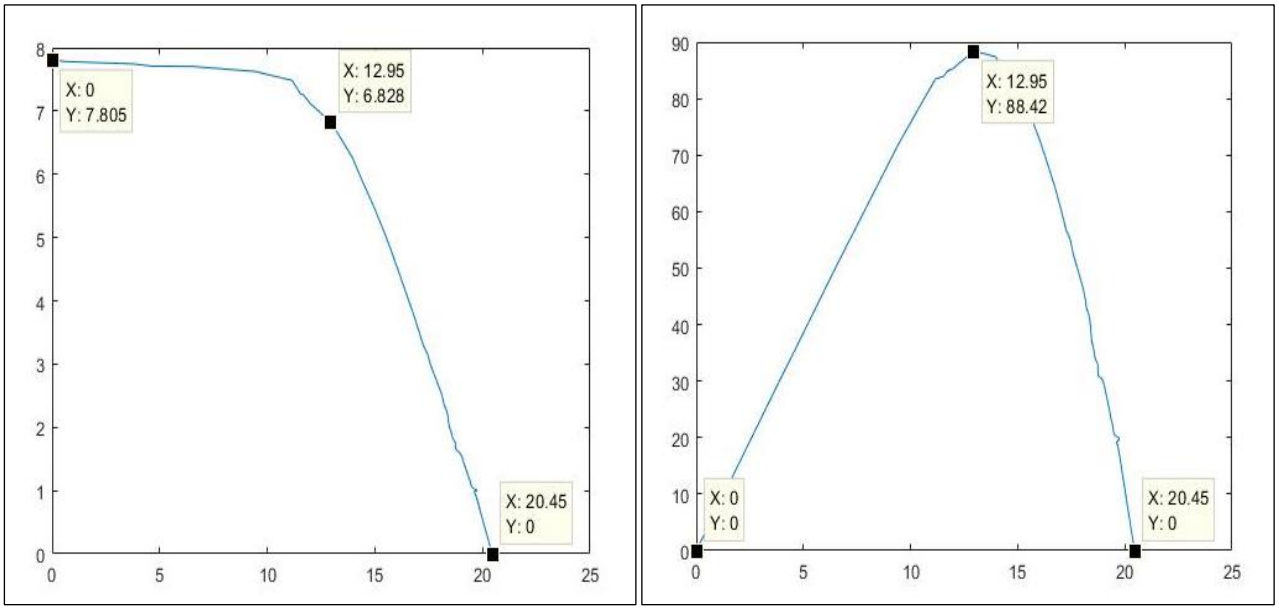

Figure 2.5: I-V and P-V curves for one module.

The cell's temperature is found using the formula 1.11 from chapter 1

$$T_{cell} = \mathrm{T}_{amb} + \left(\frac{NOCT-20}{0.8}\right) G$$

$$\mathrm{T}_{cell} = 28 + \left(\frac{45-20}{0.8}\right) 1$$

$$T_{cell} = 59.25℃$$

$$\Delta \mathrm{T} = \mathrm{T}_{\mathrm{cell}} - 25$$

$$\Delta \mathrm{T} = 34.25℃$$

Using Matlab-Simulink, the I-V and P-V curves at the same temperature using the data sheet characteristics are plotted:

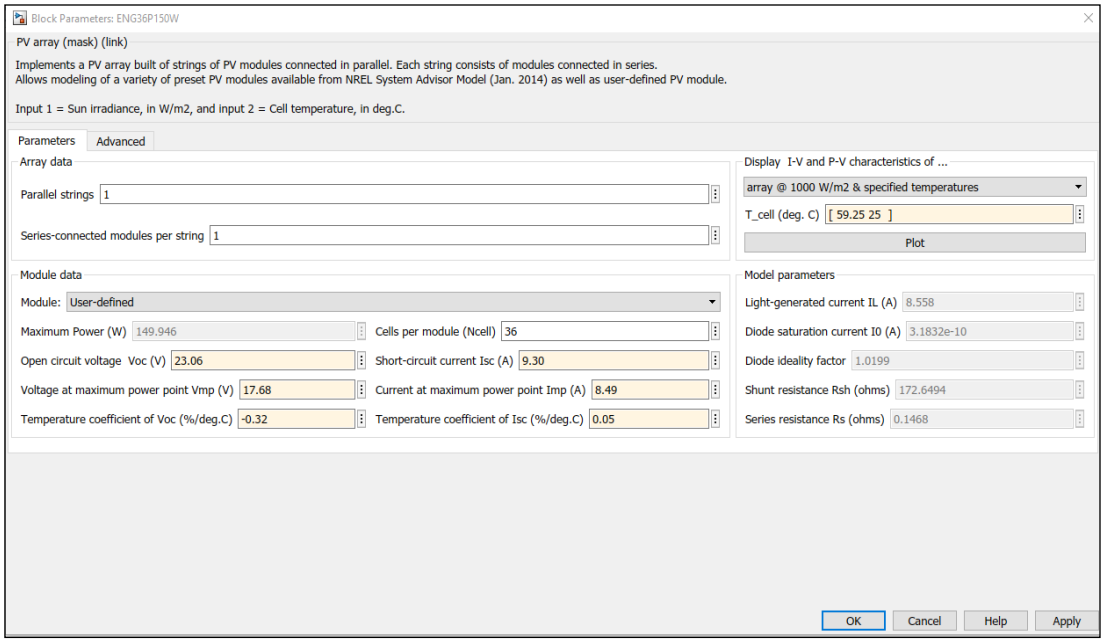

Figure 2.6: The Solar module Configuration.

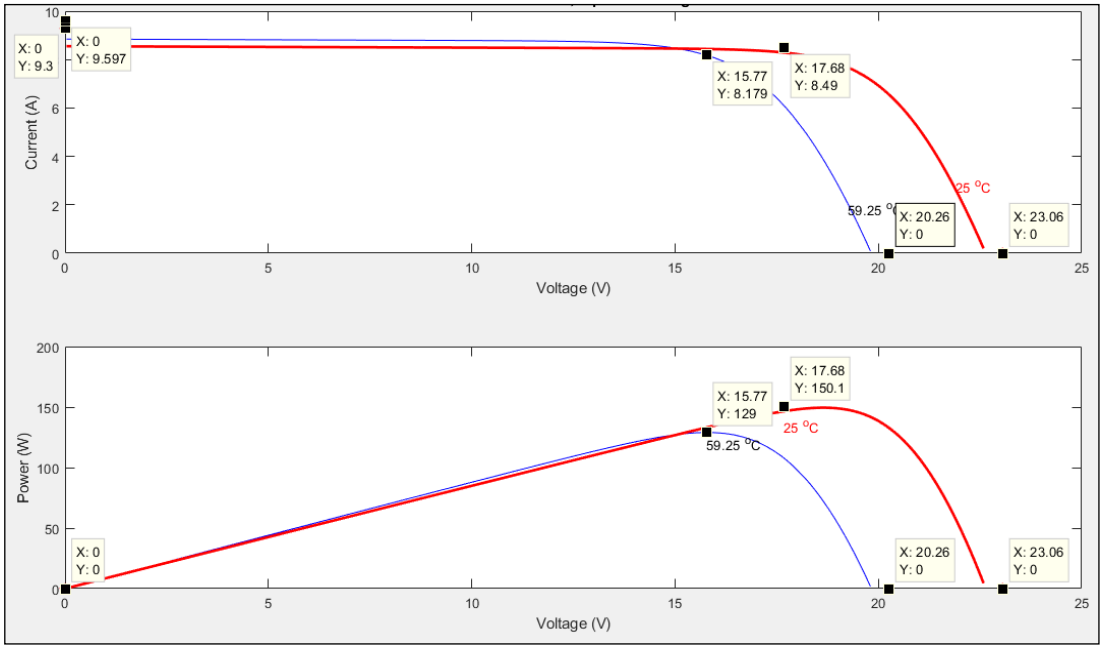

Figure 2.7: I-V and P-V curves at 25°C and 59.25°C

2.2.2 Test results analysis

The I-V and P-V curves from figures 2.2.5 and 2.2.7 illustrate a wide difference between the datasheet values and the measured values of current, voltage and power.

- Both the measured short circuit current and the measured maximum current are lower by 1.8A and 1.35 A (approximately) respectively compared to the datasheet values.
- The open circuit voltage is higher by 0.2 volt but the Maximum Voltage is lower by 2.8 V.
- The measured maximum power is 88.42W knowing that the datasheet maximum power can reach up to 129W.

From the datasheet of the modules, the STC values of V_{oc}, I_{sc} and P_{max} are calculated as follows:

$$V_{oc} = \frac{40.9/2}{(1 - 0.32\% * 34.25)} = 22.97V$$

$$I_{sc} = \frac{15.61/2}{(1 + 0.05\% * 34.25)} = 7.67A$$

$$P_{max} = \frac{88.42}{(1 - 0.45\% * 34.25)} = 104.53W$$

- The value of V_{mpp} and I_{mpp} in STC can't be calculated because of the environment.

2.3 Charge Regulator

The main task of the charge controller (regulator) is to manage the power going into the battery bank from the solar array. It ensures that the batteries are not overcharged during the day and that the power doesn't run backwards to the solar panels overnight. It also prevents the batteries from getting fully discharged because of the load consumption. There are mainly three varieties of Charge controllers: Ordinary ON or OFF control, PWM and MPPT. Their performance in a system is very different from each other. [11]

2.3.1 Ordinary ON or OFF control

Ordinary ON or OFF controllers consist of a relay that opens the charging circuit when a preset high-voltage point is reached and closes the circuit again when a preset low-voltage threshold is reached, allowing charging to continue. It is the simplest control strategy to control the charging and discharging of batteries. [12]

2.3.2 PWM charge controller

Modern charge controllers use Pulse Width Modulation (PWM) to slowly lower the amount of power applied to the batteries as they get closer and closer to full charge. This type of controller allows the batteries to be charged with less stress, extending battery life. It can also keep the batteries in a fully charged state (called “float”) indefinitely. PWM is more complex, but does not have any mechanical connections to break. [12]

2.3.3 MPPT charge controller

The main advantage of the MPPT charge controller is tracking the maximum power, since the solar array generate different values of voltage depending on the load resistance, the voltage is controlled by a DC-DC converter where the duty cycle is varied to track the Maximum Power Point (MPP). Different methods are used to approach the Maximum Power Point as:

- **Hill Climbing/Perturb and Observe (HC/P&O):** it uses the duty cycle of boost converter as the judging parameter when the task of the maximum power point tracking is implemented. When the condition dP/dV = 0 is accomplished, it means that the maximum power point has been tracked. The duty cycle in every sampling period is determined by the comparison of the power at present time and previous time. [13]
- **Incremental Conductance (IncCond):** this technique employs the slope of the PV array power characteristics to track MPP. The slope of the PV array power curve is zero at the MPP, positive when the voltage is smaller than the MPP voltage and negative when the voltage is greater than the MPP voltage. The derivative of the power of the PV module is given by [13]:

$$\frac{dI}{dV} = -\frac{I}{V} \tag{2.1}$$

- **Constant voltage:** it is the simplest MPPT control method. The operating point of the PV array is kept near the MPP by regulating the array voltage and matching it to a fixed reference voltage V_{ref}. The V_{ref} value is set equal to the VMPP (STC) or set to a fixed calculated value. [14]

The charge controller used in the implementation is MPPT T40 (see Appendix A). which has a 10% to -30% higher efficiency than the ordinary charge controller. It also has standby energy saving (more than 30% energy than ordinary controller) and a standby power consumption of only 10mA-15mA.

Figure 2.8: MPPT T40 Charge Controller.

The charge regulator settings:

- Battery float voltage: 27.6V
- Battery (under voltage) protection: 21.2V
- Battery (under voltage) recovery voltage: 25.2V

The charge regulator stops charging the batteries directly if they reach 27.6V and stops absorbing power from them when they reach 21.2V. It starts absorbing power again when they reach 25.2V.

2.4 Batteries

The battery is utilized to provide energy to the load when the PV array cannot derive enough energy at night or in a cloudy day, this function provided by the battery is called ‘‘battery’s autonomy’’.

The deep-cycle lead-acid batteries are the most suitable for solar system since they are specially designed for frequent cyclic performance. By using strong grids and specially designed active material, they offer more cyclic life.

To provide a 24V, two RITAR DC12-120 batteries are connected in series to the MPPT terminals (see Appendix B), with a capacity of 120Ah for each battery, a 12 V nominal voltage, an internal resistance of 4.5mΩ at 25℃, a wide operation temperature range: -20 to 60 ℃ and a high short circuit current of 2.22KA.

2.5 Inverter

A single-phase voltage-source inverter is an electronic device or circuitry that changes direct voltage (DC) into alternating voltage (AC). Inverters are constructed from controllable power switches (IGBT or MOSFET…) controlled according to the type of ac output waveform wanted (magnitude and frequency), however the output waveform is not sinusoidal, to ensure a sinusoidal signal, modulating techniques are used to control the amount of time and the sequence used to switch the power valves on and off. The modulating techniques most used are: sinusoidal pulse width modulation (SPWM), the space-vector (SV) technique and the selective-harmonic-elimination (SHE) technique. There are many different single-phase inverter topologies. Based on the switch leg numbers, inverters can be sorted as half-bridge inverters or full-bridge (H-bridge) inverters. [15]

2.5.1 Half-bridge inverter

The Half bridge inverter consists of two switches and two capacitors. For each half of the period a switch is on and the other one is off. The two switches should not be on at the same time. [15]

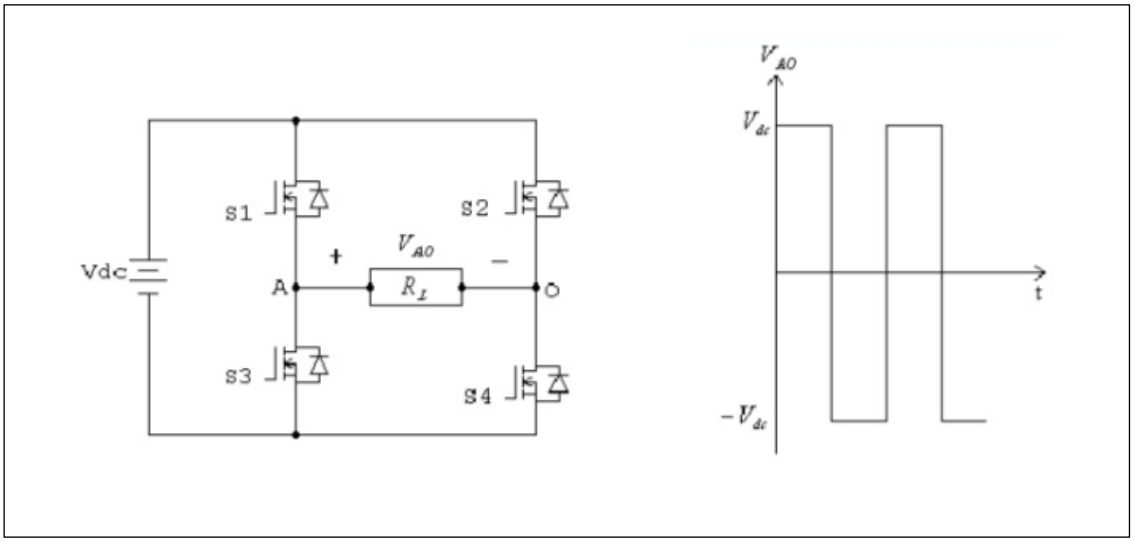

Figure 2.9a: Full bridge inverter and its corresponding output

2.5.2 Full-bridge inverter

The full-bridge inverter consists of four switches. The operation is divided into two identical periods where the switches S1 and S4 are on in the first half of the period while switch S2 and S3 are off. In the second half of the period, switches S1 and S4 turn off and switches S2 and S3 turn on. [15]

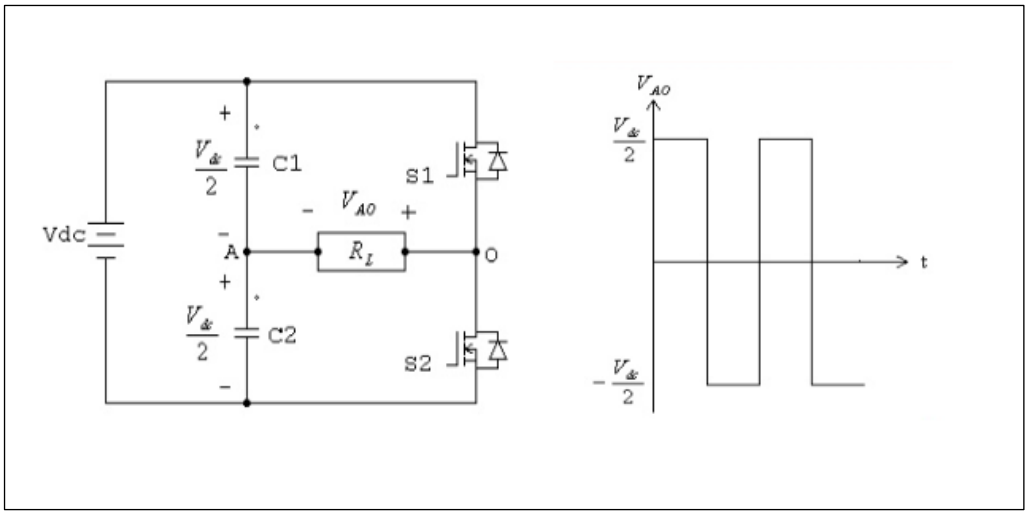

Figure 2.9b: Half bridge inverter and its corresponding output.

Phoenix Inverter 24/800 is used in the implementation (see Appendix C). it's a single-phase inverter which can produce a true sinewave AC voltage with an RMS value of 230V and a frequency of 50Hz starting from a DC voltage of 18.4 to 34.0 V and producing a maximum power of 800W.

Figure 2.10: Pure Sinewave Inverter.

2.6 Load

Loads are the power consuming units of the PV system. There are two types of loads (ac and dc) depending on the type of electrical power that they require for their operation. [16] For this implementation both ones are accepted.

Eight resistive lamps are connected in series to the inverter, the total load impedance is 267.2Ω where each lamp has a resistance of 33.4Ω.

2.7 Data acquisition system

The data acquisition system is supposed to measure the data of the irradiance, temperature, current and voltage; then send them through WIFI to be processed using Lab-View Software. The system consists of two circuits: the first one is fixed on the PV array

to measure the irradiance and temperature using a photodiode and an IC temperature sensor (LM 35), then send them to the main circuit. The latter is composed of Hall-effect and voltage measurement sensors which are responsible for measuring the current and the voltage respectively.

Two ESP32 microcontrollers are used to transfer the data from the first circuit to the main one then to the laptop through through WIFI.

Unfortunately, the system didn't work as desired, and couldn't be fixed because of the lack in time and material.

To solve this problem, the data is measured manually using a solar power meter, thermometer and multimeters.

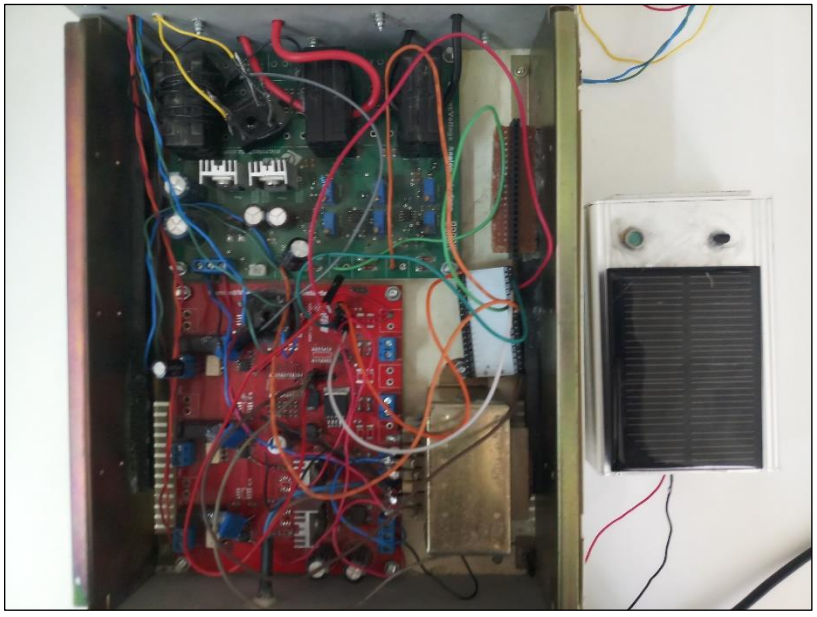

Figure 2.11: Data acquisition system.

2.8 Solar Power Meter

TES-1333 Solar Power Meter is used to measure the amount of solar irradiance throughout the day; it can display four digits with a Max indication of 1999 W/m², a resolution of 0.1W/m², a high accuracy within ±10W/m² and data hold which has a maximum memory of 99 sets.

Figure 2.12: TES-1333 Solar Power Meter.

2.9 Thermometer

TES-1310Thermometer is used to measure the ambient temperature around the solar panels; it can display 4 digits with a switchable Resolution of 0.1° /1.0 °, a range of -50℃ to 1300℃, a high accuracy within 0.2% and a data hold function.

Figure 2.13: TES-1310Thermometer.

2.10 Conclusion

In this chapter, the main implementation components are introduced, the PV modules and the batteries are responsible for providing power to the inverter with the help of the MPPT charge controller that control the power flow.

An identification test is done to determine more accurate parameters, since the ones given by the datasheet are not accurate. The test demonstrates a wide difference in the voltage and current values at specific conditions; where the irradiance is around 1000w/m² and the ambient temperature is 28℃, which increases the temperature of the cells to 59.25℃.

Chapter Three

IMPLEMENTATION AND MEASUREMENT RESULTS

3.1 Introduction

The implementation and the measurement results are discussed in this chapter. First of all, a diagram of the implementation is represented and demonstrated, then a set of graphs represent the results of the change in irradiance, temperature, current, voltage and power versus time. The graphs are plotted and described individually.

The PV array and Batteries are connected to the MPPT charge controller through two Circuit Breakers (16A), then the MPPT provides power to the Single-Phase Inverter which converts the DC voltage into AC voltage with an RMS value of 230V. A load of eight lamps is connected to the inverters output terminals. Four multimeters are used, two of them are connected to the PV array and batteries positive terminals respectively to measure the output current. The other two are connected to the PV array and batteries to measure the voltage.

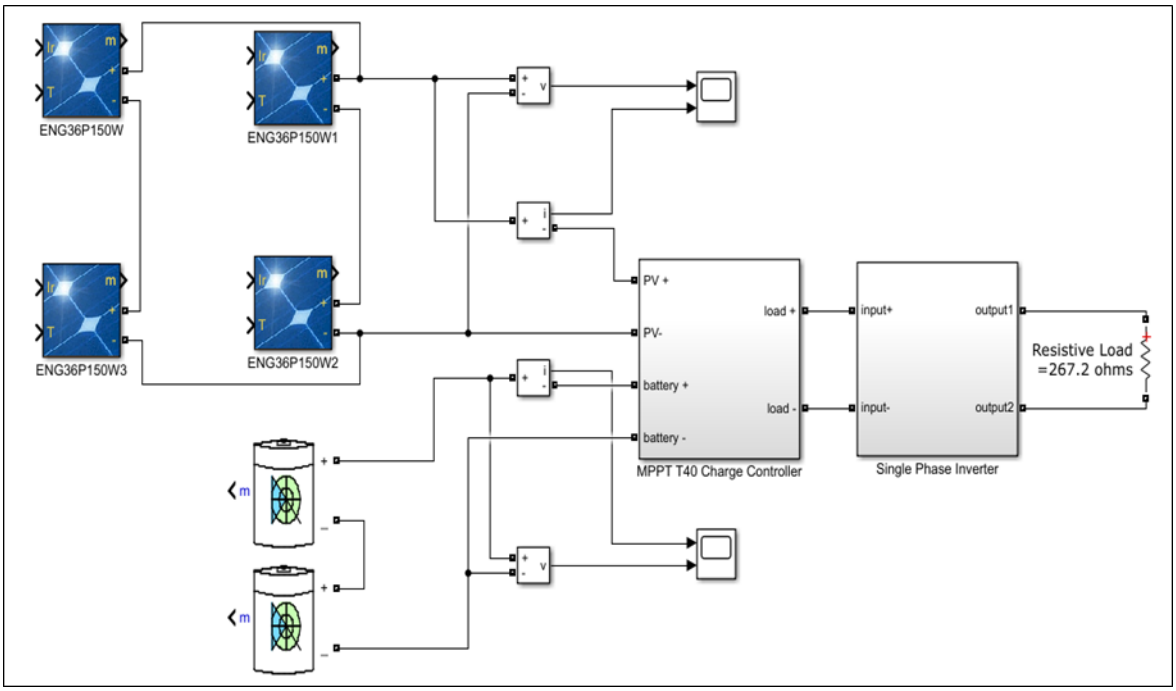

Figure 3.1: Overall system circuit diagram.

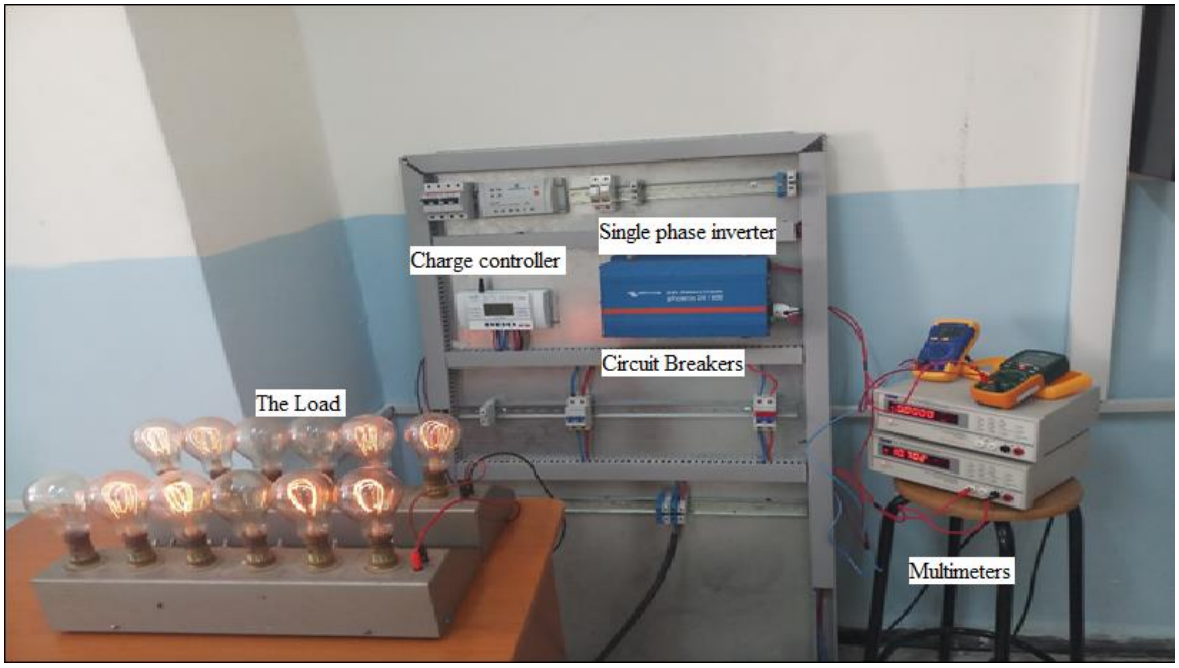

Figure 3.2: The implemented circuit used in the study.

The values of temperature and irradiance are measured simultaneously with the values of current and voltage every five minutes from morning (7:00AM) to evening (5:00 PM) for fifteen days of the month of May.

3.2 Measurement results

The data of two days is taken as a sample to study in this chapter, a sunny and a cloudy day (May the 15th2019 and May the 21st 2019 respectively).

Due to the effect of irradiance, the temperature of the cell increases to reach a peak value at noon in sunny days. Figures 3.3a and 3.3b illustrate the difference between the ambient temperature and the cell temperature at a sunny and a cloudy day.

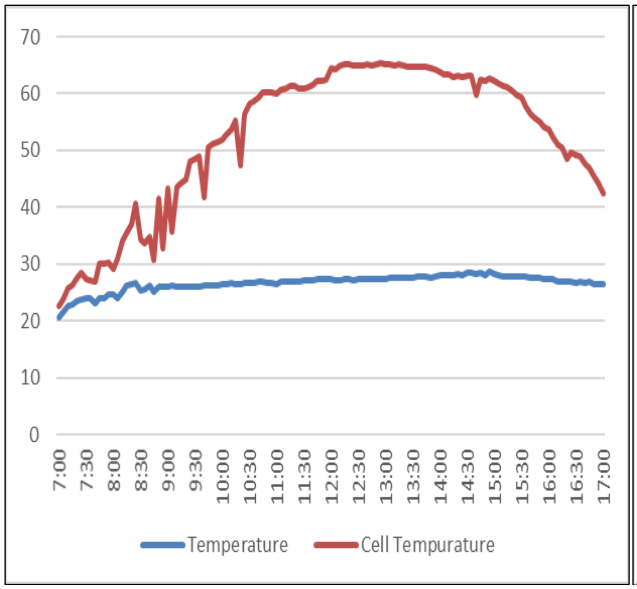

Figure 3.3a: Cell temperature and ambient temperature for a sunny day.

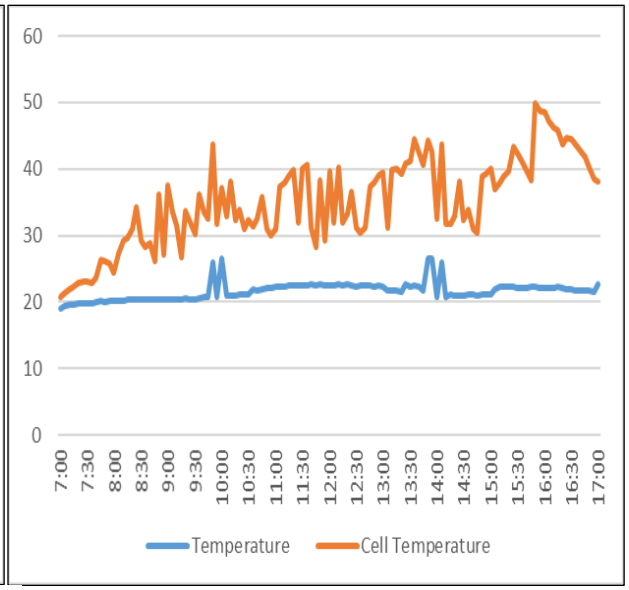

Figure 3.3b: Cell temperature and ambient temperature for a cloudy day.

It is clear that the irradiance affects the cell temperature directly. In the sunny day, T_{cell} increases with the increase of irradiance, while in the cloudy day, T_{cell} keeps changing due to the change in irradiance (the sun hides behind the clouds).

The change in cell temperature affects the open circuit voltage, however the MPPT T40 uses the constant voltage method, which leads to fixed voltage values. The MPPT charge controller first calculates the MPP voltage, takes it as a reference and tries to keep it fixed.

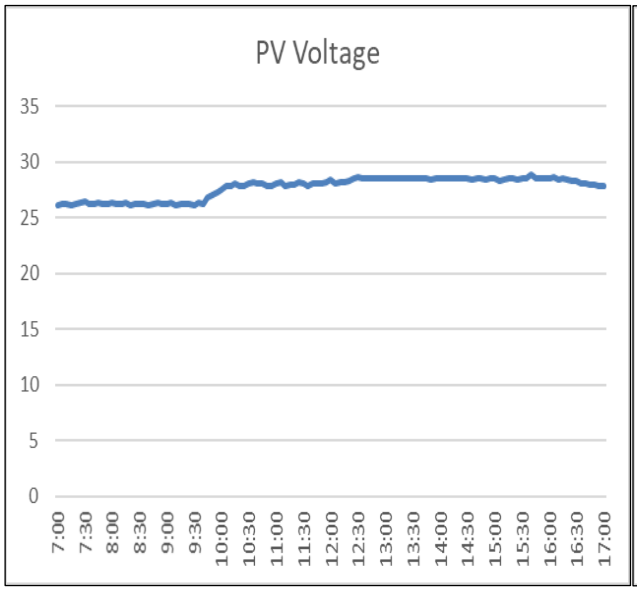

Figure 3.4a: The PV voltage changes for a sunny day.

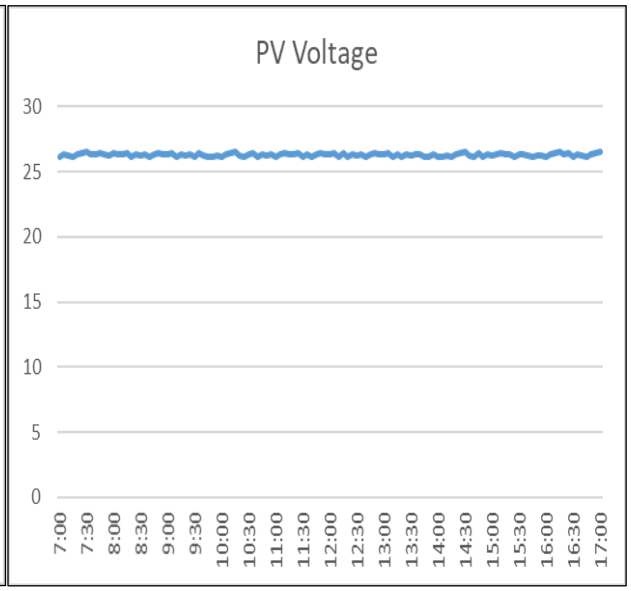

Figure 3.4b: The PV voltage changes for a cloudy day.

The figures 3.4a and 3.4b prove that the MPPT T40 utilizes the constant voltage method to identify the MPP, because in both cases the voltage is around 26V. The charge controller calculates the first value of the MPP corresponding to the temperature at that moment, then tries to maintain the voltage fixed.

Since the voltage is approximately stable, the main factor controlling the power provided by the PV array is the current, which changes due to the change in the irradiance.

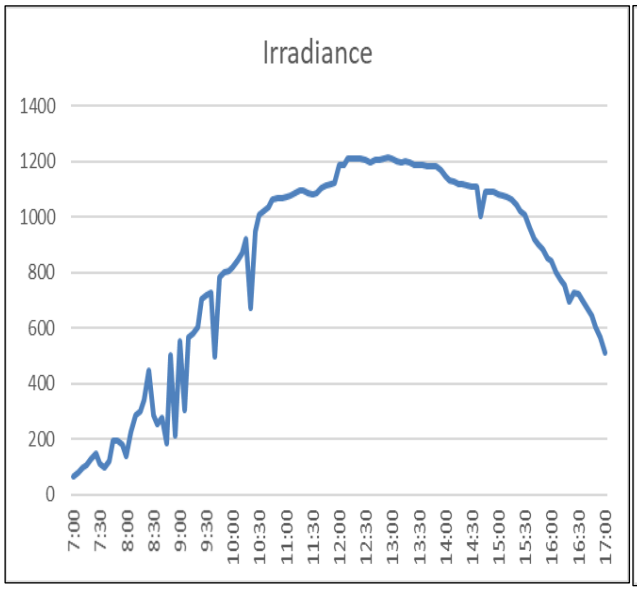

Figure 3.5a: The irradiance changes for a sunny day.

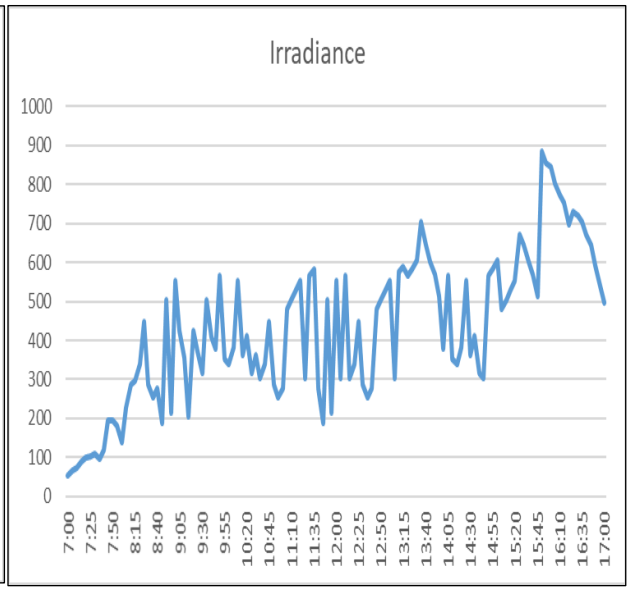

Figure 3.5b: The irradiance changes for a cloudy day.

Figure 3.5a and 3.5b demonstrate how the weather affects the irradiance, which keeps changing in cloudy days due to the change in the density of the clouds.

In sunny days, the irradiance exceeds 1200W/m². However, in cloudy days it keeps varying between 300 to 600W/m².

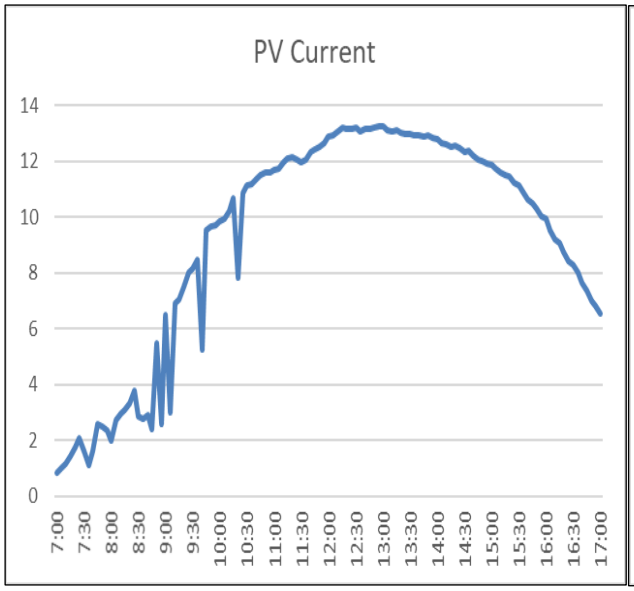

Figure 3.6a: The PV current change for a sunny day.

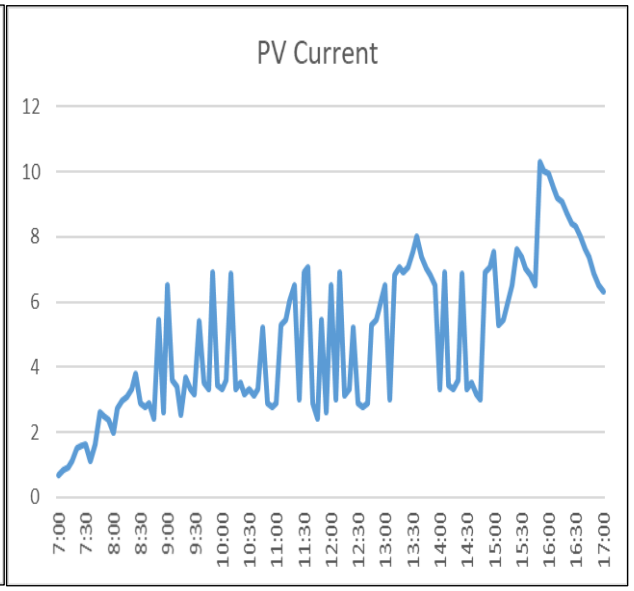

Figure 3.6b: The PV current change for a cloudy day.

Even though in sunny days the current provided by the PV array exceeds thirteen amperes, in cloudy days the current keeps varying between two to seven amperes and exceeds it for small durations of time when the clouds stop hiding the sun or partially hide it.

In sunny days the PV array generates more current than what the inverter requires to supply the load. Therefore, the MPPT charge controller charges the batteries with the remaining current. i.e. Around 4A when the current reaches its peak values. However, in cloudy days the current generated by the PV array can't satisfy the power requirement of the inverter. Thus, the MPPT charge controller starts absorbing current from the batteries.

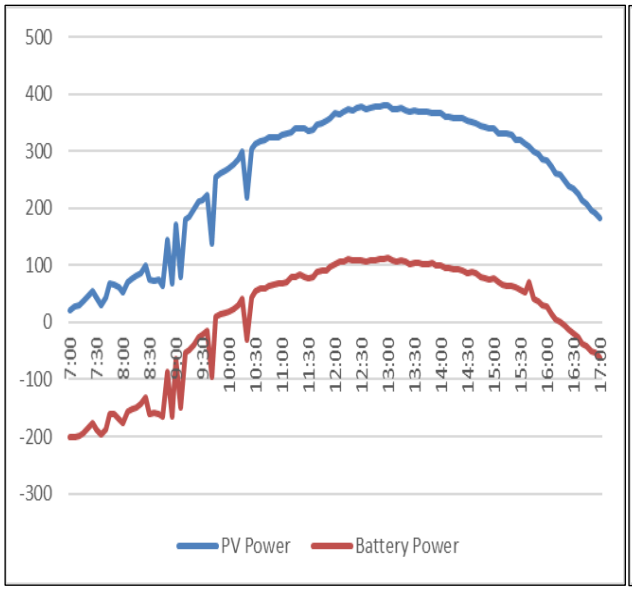

Figure 3.7a: The power flow for a sunny day.

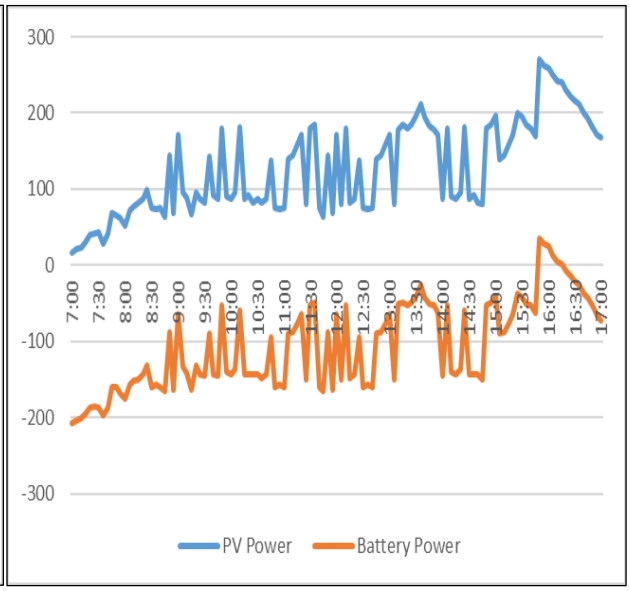

Figure 3.7b: The power flow for a cloudy day

Since power is the product of the current and the voltage (the voltage is approximately stable), the change in power is propotional to the change in current where the main factor controlling the power (and the current) change is the irradiance.

The power generated by the PV array varies from 25 W to reach a peak of 384W in a sunny day, but in cloudy days the power keeps varying from 20W to 200W only.

The inverter generates a signal output of 230 Vrms and 0.86 Arms with a power of 200W, and to generate this signal the MPPT absorbs around 240W from the PV array and the batteries to supply the inverter.

The power absorbed or delevired to the batteries depends on the power generated by the PV array.

3.3 Conclusion

In this chapter the implementation of the project and the measurement results are clarified. As a start, the fixed voltage at the PV array output proves that the MPPT T40 charge controller utilizes the constant voltage method, where it calculates the first value of MPP, then takes its voltage as a reference and tries to keep it constant.

Secondly, processing the data collected yields information on the way the current changes (proportionally to the irradiance) and how the clouds affect it.

Finally, the study shows how the power flow changes with time, and what's the maximum power the PV array can generate in the site at the best conditions in the month of May, which are 1267W/m² irradiance, 27℃ and a power of 384 W.

Chapter Four

DATA ANALYSIS USING WEIBULL++

4.1 Introduction

The collected data i.e. Irradiance, temperature and power are processed using Weibull++ software, where the Kolmogorov–Smirnov test is applied to the collected data to determine which distribution it follows. Based on the distribution and its parameters, the mean value, pdf and cdf of the data are deduced.

4.2 Weibull++ study and analysis

The study took place over the span of 15 days, some of which were sunny while others were cloudy. The data of sunny days is similar and the data of cloudy days is similar too. Therefore, in this study only two days are chosen, one day is sunny and the other is cloudy.

In order for the data to be relevant it should be confirmed by the Kolmogorov-Smirnov test where it follows the probability line and stay within the confidence bounds.

For our purposes, the irradiance data measured during a sunny and a cloudy day from the sample period are used to define the fitting distributions, their parameters and the mean values. The figures 4.1 and 4.2 show the different distributions.

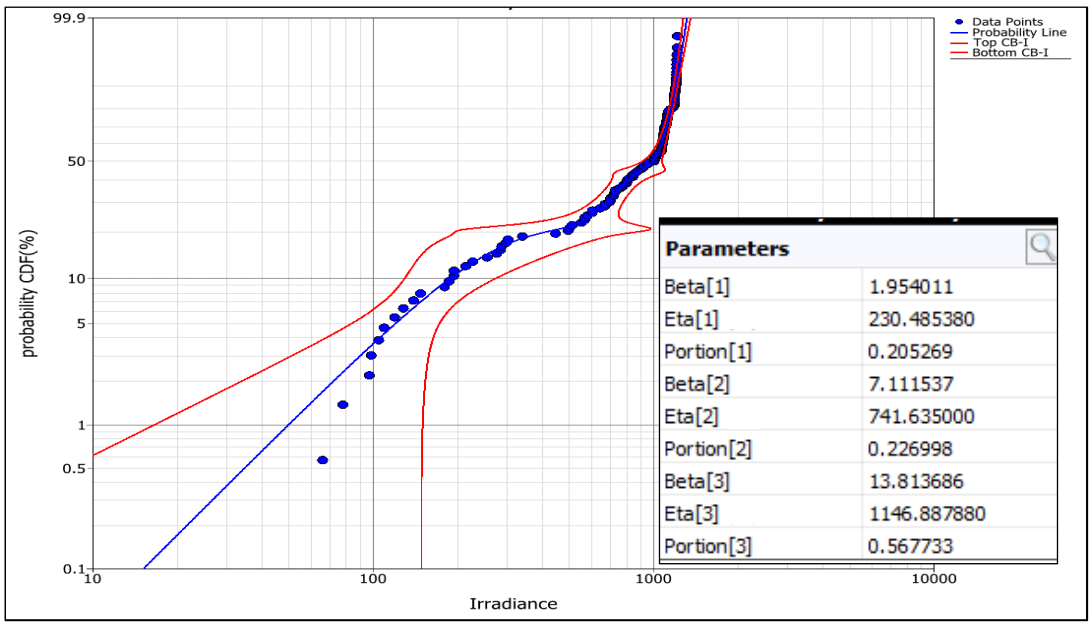

Figure 4.1: The irradiance data cdf for a sunny day.

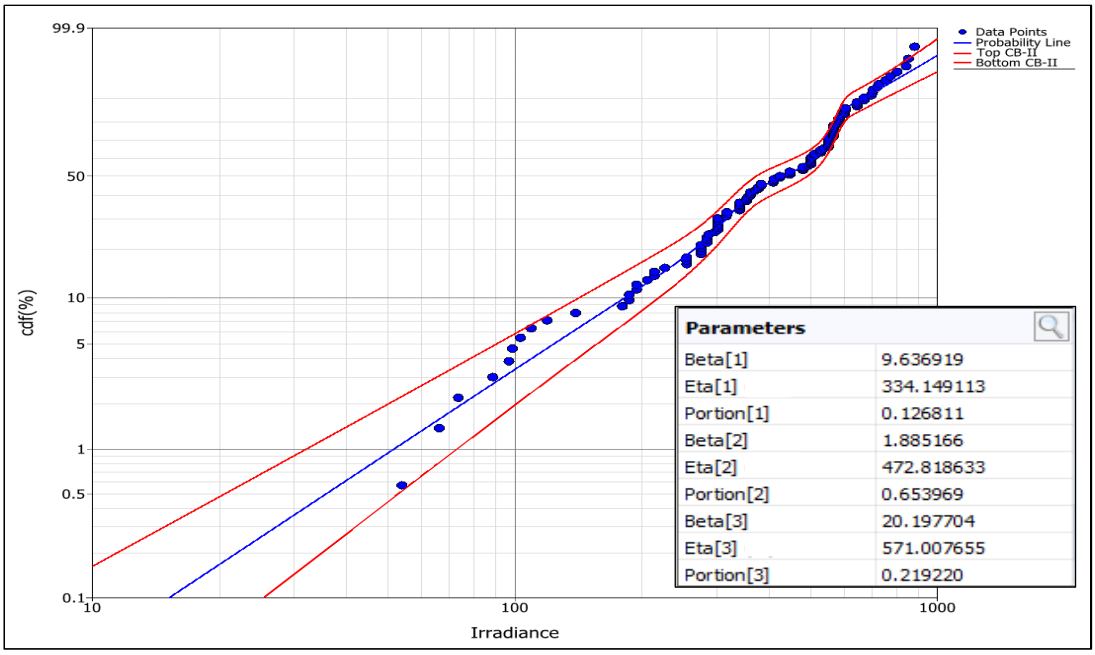

Figure 4.2: The irradiance cdf and its parameters for a cloudy day.

The irradiance data of a sunny and a cloudy day are fitted with a three subpopulations mixed Weibull distribution. The irradiance mean value for the sunny day is 826.64 w/m^2whereas that of the cloudy day is 436.58 w/m^2. The parameters are used to define their respective cdfs according to equation 1.23:

$$F_{sunny}(x) = 0.20\left[1 - e^{-(\frac{x}{230})^{1.95}}\right] + 0.23\left[1 - e^{-(\frac{x}{741.6})^{7.1}}\right] + 0.57\left[1 - e^{-(\frac{x}{1147})^{13.8}}\right] \quad (4.1)$$

$$F_{cloudy}(x) = 0.13\left[1 - e^{-(\frac{x}{334})^{9.64}}\right] + 0.65\left[1 - e^{-(\frac{x}{473})^{1.9}}\right] + 0.22\left[1 - e^{-(\frac{x}{571})^{20.1}}\right] \quad (4.2)$$

Where x represents the irradiance.

The same procedure using the temperature data of a sunny and a cloudy day is repeated. See the figures 4.3 and 4.4:

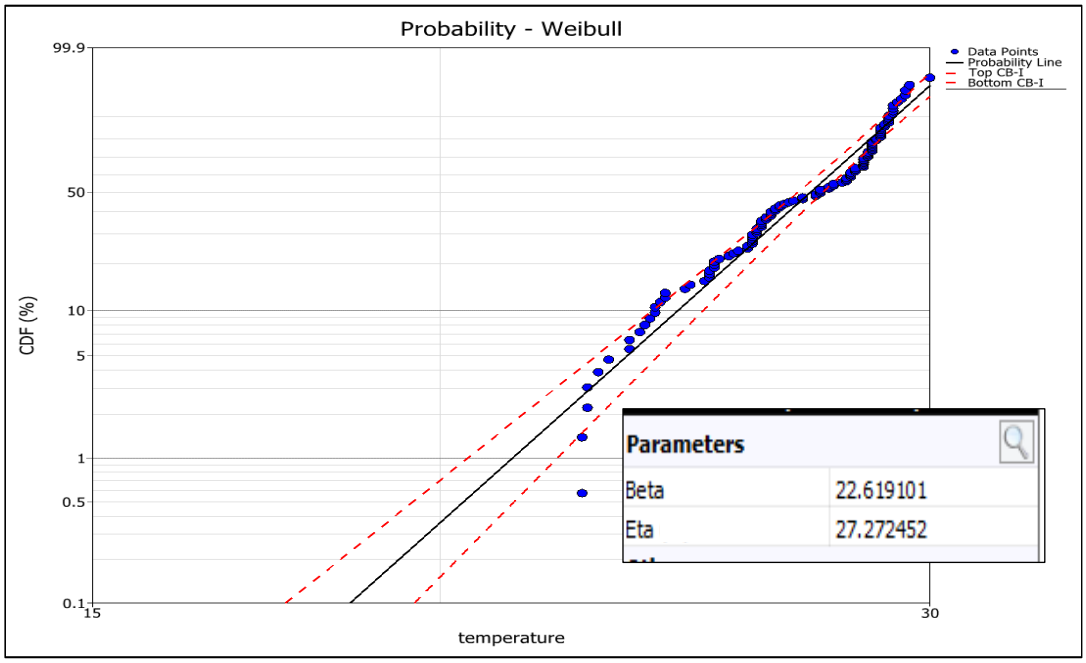

Figure 4.3: The temperature cdf and its parameters for a sunny day.

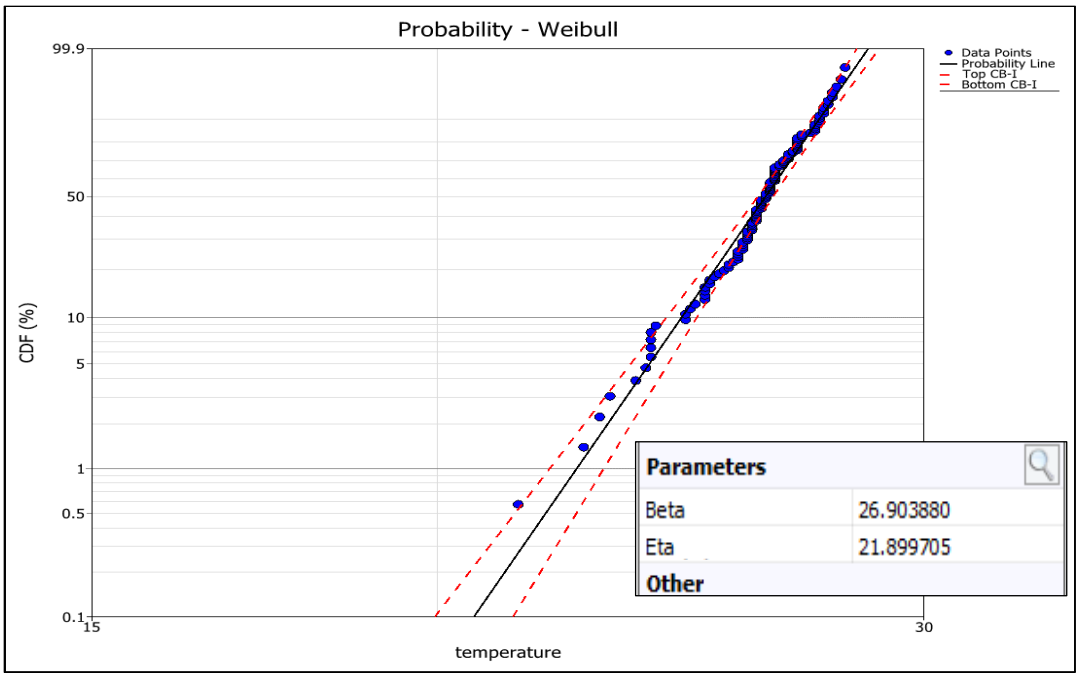

Figure 4.4: The temperature cdf and its parameters for a cloudy day.

The temperature data of a sunny and a cloudy day are fitted with a Weibull distribution. The temperature mean value for the sunny day is 26.3℃ and the mean value of cloudy day is 22.5℃. The parameters are used to define their respective cdfs according to equation 1.21:

$$F_{sunny}(x) = 1 - e^{-\left(\frac{x}{27.3}\right)^{22.6}} \quad (4.3)$$

$$F_{cloudy}(x) = 1 - e^{-\left(\frac{x}{21.9}\right)^{26.9}} \quad (4.4)$$

Where x represents the temperature.

After that, the same procedure is used with the power data of a sunny and a cloudy day. See the figures 4.5 and 4.6.

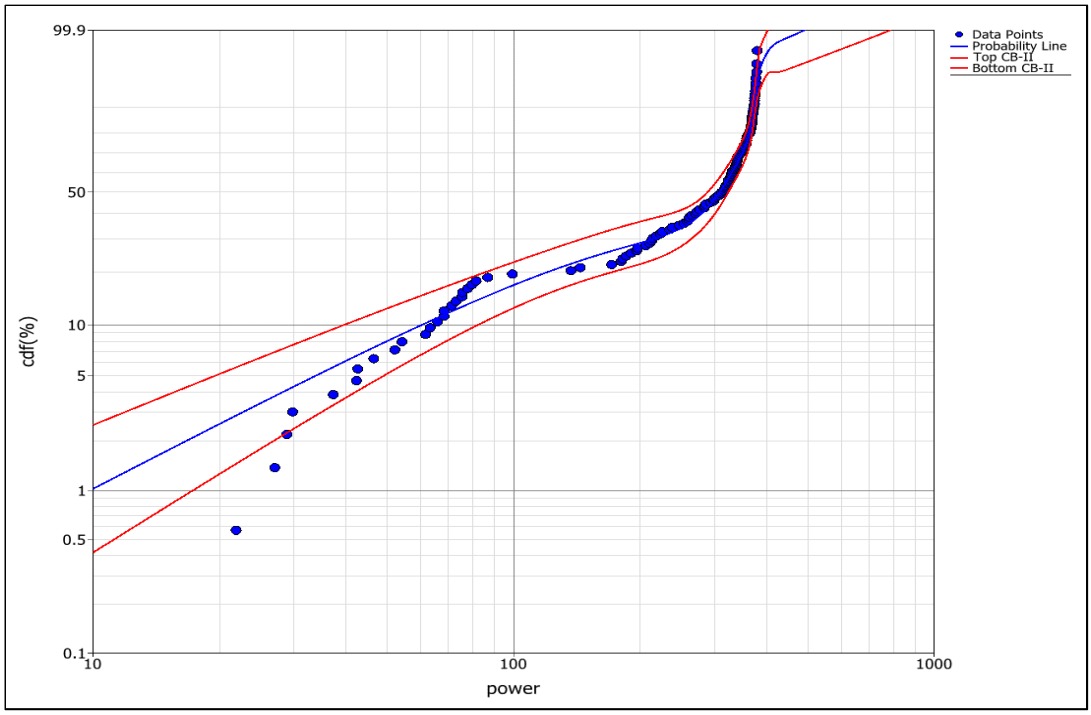

Figure 4.5*:* The power cdf for a sunny day.

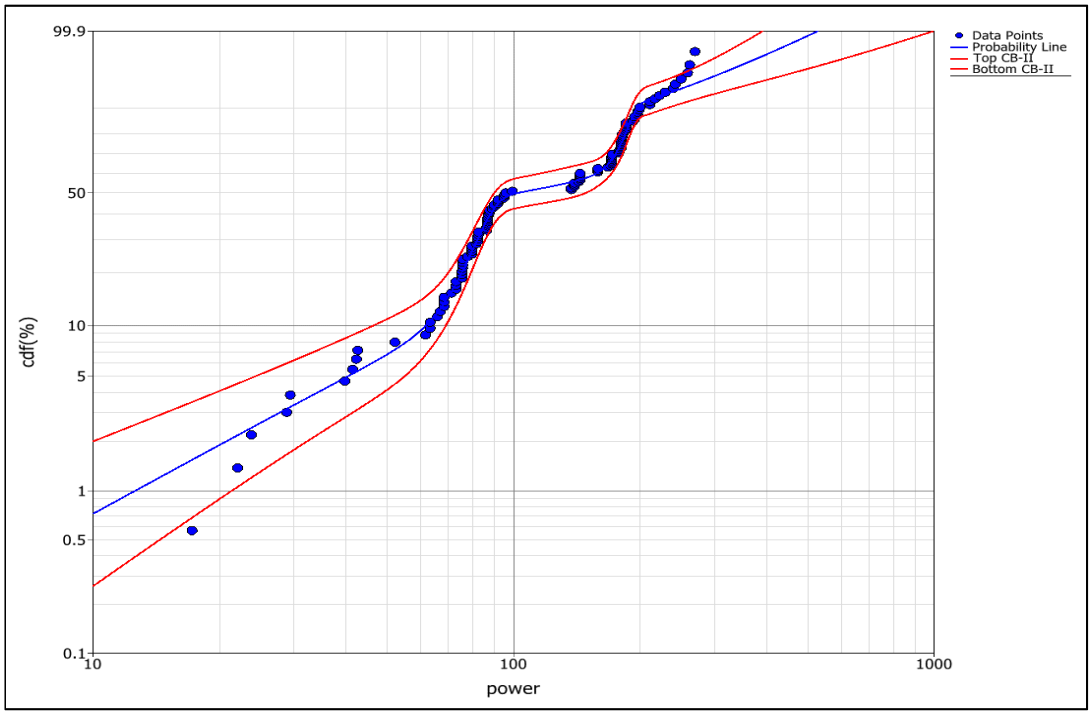

Figure 4.6: The power cdf for a cloudy day.

The power data of a sunny and a cloudy day are fitted with a four subpopulations mixed Weibull distribution. The power mean value for the sunny day is 265.3W whereas that of the cloudy day is 128.9W.

As a result, the mean value change in temperature between a sunny and a cloudy day is small (3.8℃). Chapter three explained that the change in temperature does not affect the performance of the system due to the constant voltage method used by the MPPT charge controller. Therefore, the performance of the system is affected by irradiance only. The mean value change in irradiance is about 390W/m^2, which translates to a change in power of 137W.

The parameters of power distributions are shown in the table 4.1:

Table 4.1: The cdf parameters of the power data.

Parameters	Sunny	Cloudy
Beta (1)	2.84	2.9
Eta (1)	72.3	35.4
Portion (1)	0.21	0.07
Beta (2)	12.0	9.2
Eta (2)	150	84.4
Portion (2)	0.107	0.40
Beta (3)	6.25	33.9
Eta (3)	288	181
Portion (3)	0.418	0.174
Beta (4)	34.9	3.98
Eta (4)	341	193.9
Portion (4)	0.265	0.347

The cdf equations according to their parameters:

$$F_{sunny}(x) = 0.21\left[1 - e^{-(\frac{x}{72.3})^{2.84}}\right] + 0.107\left[1 - e^{-(\frac{x}{150})^{12.0}}\right] + 0.418\left[1 - e^{-(\frac{x}{288})^{6.25}}\right] + 0.265\left[1 - e^{-(\frac{x}{341})^{34.9}}\right] \quad (4.5)$$

$$F_{cloudy}(x) = 0.07\left[1 - e^{-(\frac{x}{35.4})^{2.9}}\right] + 0.40\left[1 - e^{-(\frac{x}{84.4})^{9.2}}\right] + 0.174\left[1 - e^{-(\frac{x}{181})^{33.9}}\right] + 0.347\left[1 - e^{-(\frac{x}{193.9})^{3.98}}\right] \quad (4.6)$$

Where x represents the power.

Assuming that the weather conditions are known (i.e. temperature, Sunny/Cloudy day) from the experiment, the relevant distribution of power, its parameters and its cdf that correspond to the data allow us to determine the powers probability during that day.

Equations 4.5 and 4.6 are used to calculate the cdf for a given power data, as the table 4.2 illustrate.

Table 4.2: The cdf of different power values.

Sunny day		Cloudy day	
X	F(x)	x	F(x)
50	0.062	50	0.07
100	0.191	80	0.266
200	0.358	100	0.492
300	0.623	150	0.577
400	1	200	1

One of the pdf properties is defined as: [17]

$$P(x_1 < x \leq x_2) = F(x_2) - F(x_1) \quad (4.7)$$

This equation can be used to calculate the probability of the power interval during a sunny and a cloudy day. The figures 4.7 and 4.8 show the intervals and their corresponding probabilities.

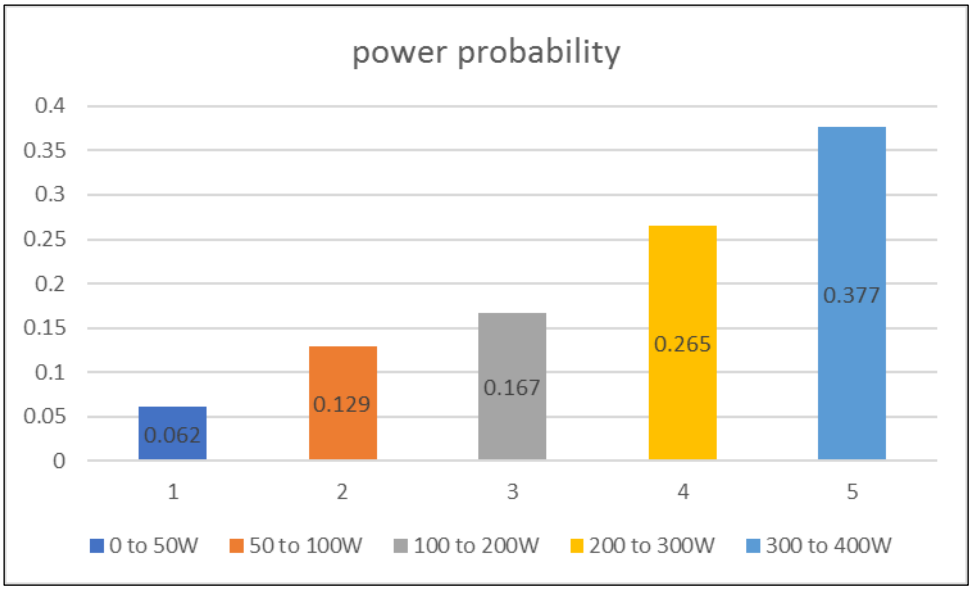

Figure 4.7: The power intervals probability during a sunny day.

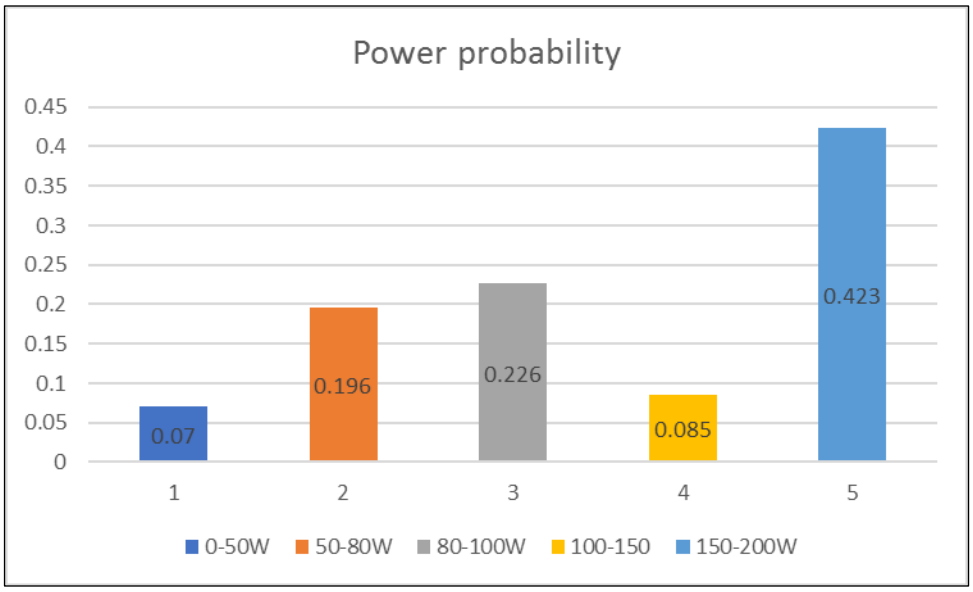

Figure 4.8: The power intervals probability during a cloudy day.

The same procedure is used to identify the power probability that the PV array can generate during a sunny day or cloudy day. For example, if the system requires 200W to operate, then according to the figure 4.8, the power probability of powering the system from the PV array is 0.642 in a sunny day. Therefore, the probability of using batteries as backup to operate the system is 0.358.

Finally, repeating the same procedure using the all days data of the sample period. See figures 4.9, 4.10 and 4.11.

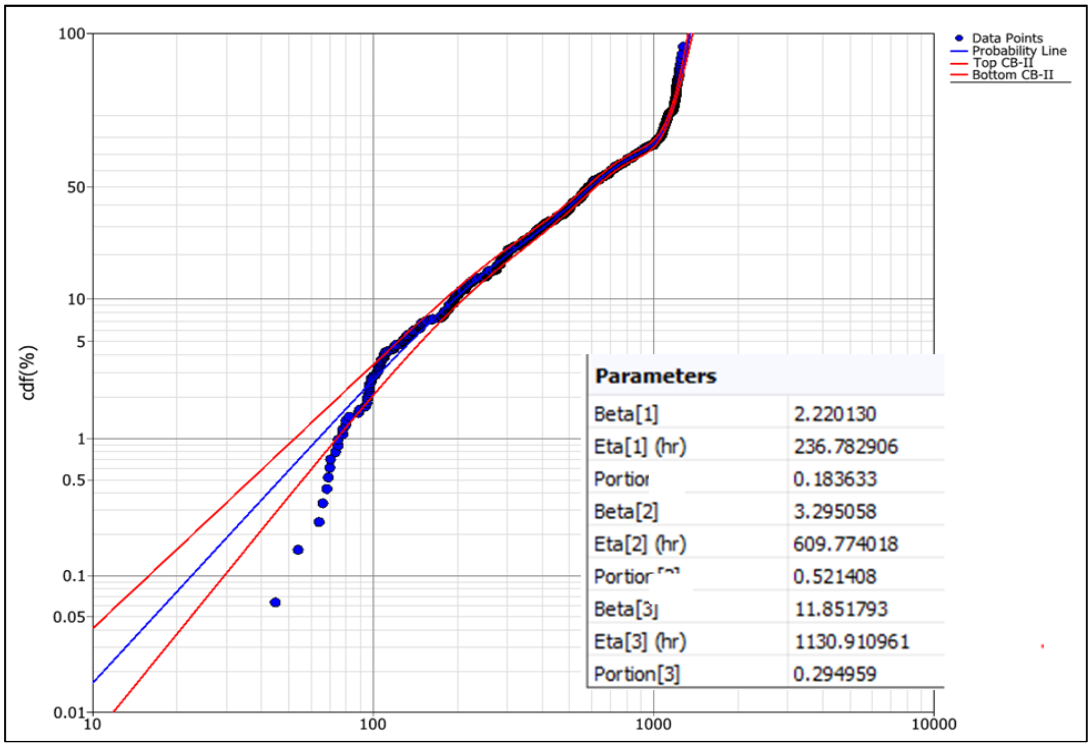

Figure 4.9*:* The irradiance cdf and its parameters for all the sample period.

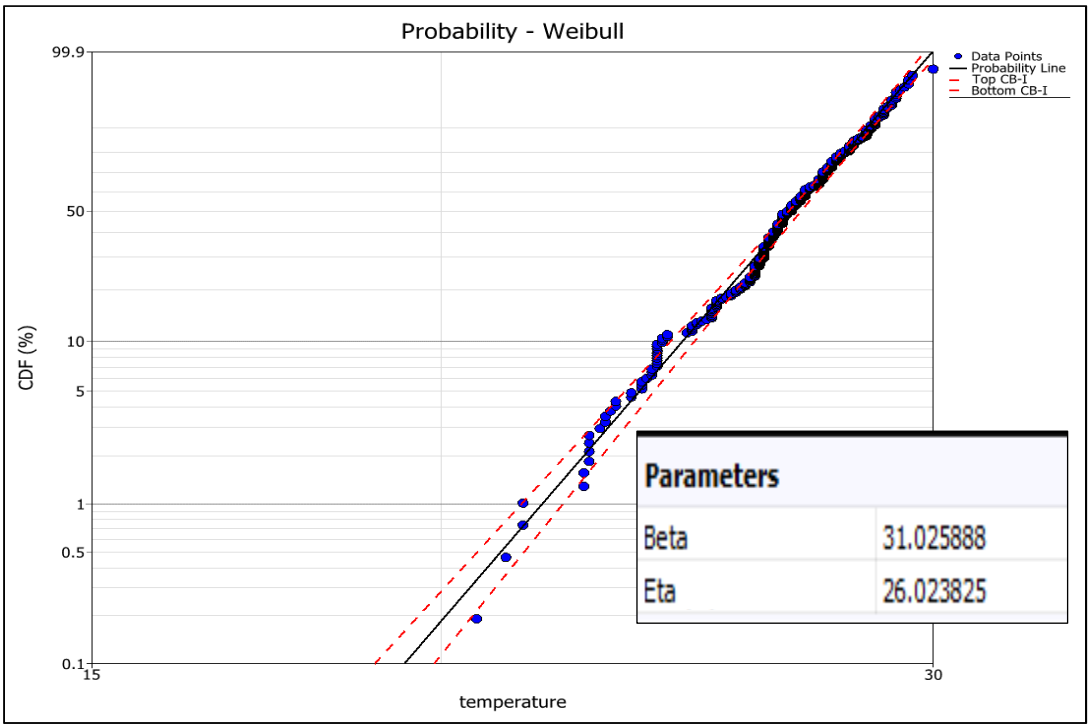

Figure 4.10: The temperature cdf and its parameters for all the sample period.

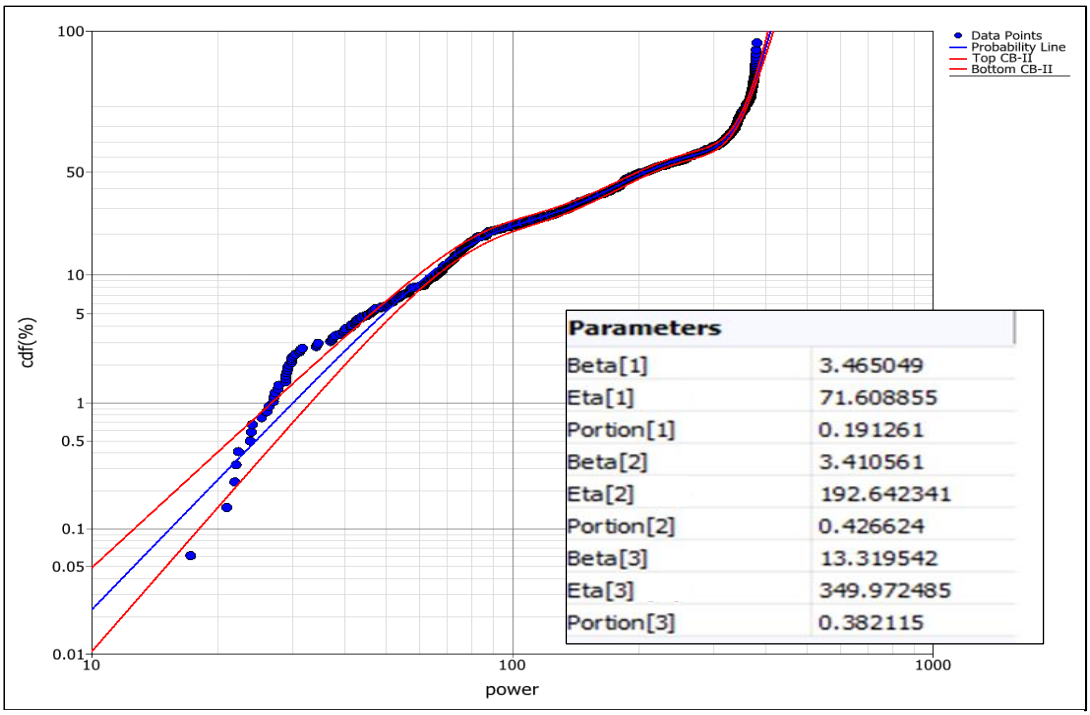

Figure 4.11: The power cdf and its parameters for all the sample period.

The irradiance data of all the sample period is fitted with three subpopulation mixed Weibull distribution. The irradiance mean value is 701.60W/m^2. The cdf equation for irradiance is:

$$F(\mathrm{x}) = 0.18\left[1 - \mathrm{e}^{-(\frac{\mathrm{x}}{237})^{2.22}}\right] + 0.52\left[1 - \mathrm{e}^{-(\frac{\mathrm{x}}{610})^{3.3}}\right] + 0.30\left[1 - \mathrm{e}^{-(\frac{\mathrm{x}}{1130})^{11.8}}\right] \quad (4.8)$$

Where x represents the irradiance.

The temperature data of all the sample period is fitted with Weibull distribution. The temperature mean value is 25.04℃. The cdf equation for temperature is:

$$\mathrm{F}(\mathrm{x}) = 1 - \mathrm{e}^{-\left(\frac{\mathrm{x}}{26.0}\right)^{31.02}} \quad (4.9)$$

Where x represents the temperature.

The power data of all the sample period is fitted with three subpopulation Weibull distribution. The power mean value is 230.9W. The cdf equation for power is:

$$F(x) = 0.29\left[1 - e^{-(\frac{x}{71.6})^{3.46}}\right] + 0.43\left[1 - e^{-(\frac{x}{192})^{3.41}}\right] + 0.38\left[1 - e^{-(\frac{x}{350})^{13.3}}\right] \quad (4.10)$$

Where x represents the power.

It is also possible to write the equation of the power probability density function of all the sample period according to the equation 1.20.

$$f(x) = 0.014\left(\frac{x}{71.6}\right)^{2.46} e^{-\left(\frac{x}{71.6}\right)^{3.46}} + 0.008\left(\frac{x}{192}\right)^{2.41} e^{-\left(\frac{x}{192}\right)^{3.41}}$$

$$+0.014(\frac{x}{350})^{12.3} e^{-(\frac{x}{350})^{13.3}} \quad (4.11)$$

Where x represents the power.

Weibull++ is used to plot the power probability density function of all the sample period. See figure bellow.

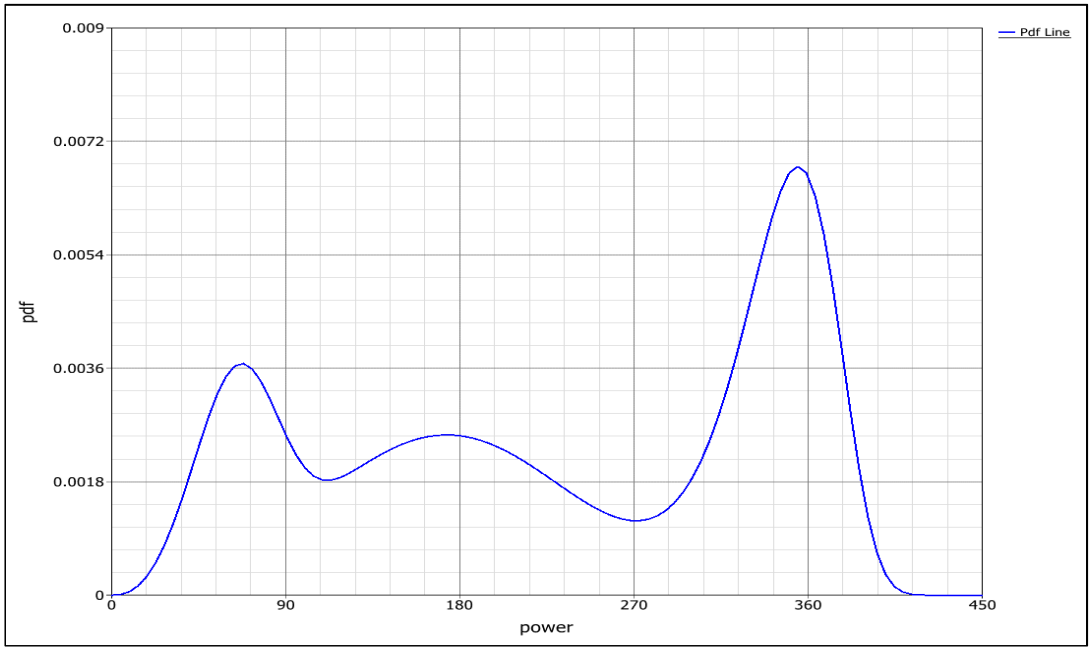

Figure 4.12: The power data pdf for all the sample period

.

4.3 Conclusion

The data used in this study is the irradiance, temperature and power. Weibull++ software is used to define which distribution the data measured follows. The parameters of distribution, the mean value, the cumulative density function (cdf) and the probability density function (pdf) of the data are determined.

The power data are divided into intervals, then the probability of each interval is calculated using its cdf. The resulting probabilities can be used to predict the power generated by the system through that day.

GENERAL CONCLUSION

General Conclusion

In order to study the data distribution of any PV system. Collection of data for the longest time possible is necessary to make the results more accurate. In this project, electrical parameters of a 600W system are recorded during the month of May for fifteen days, ten hours daily and each five minutes.

We faced many problems when collecting the data starting with the failure of the data acquisition circuit. Also, the constant voltage method used by the MPPT made the temperature effects on the system unclear.

After implementing the system, we tried to identify the real parameters of the PV modules. Unfortunately, because of the temperature, the MPP voltage and current at STC couldn't be calculated.

A sunny and a cloudy day are taken as samples in this study. After calculating the power generated by the PV array, Weibull++ software is used to determine which distribution the data is following and its mean value. According to the parameters of the distribution, a cdf is concluded. Which allowed us to calculate the probability of power intervals and starting from these probabilities, the consumers can have an idea about the amount of power that a system can generate at different conditions (time of the year, weather conditions and the site), where they will have more information than the datasheet can provide.

For future works the data should be collected automatically, the duration between each value should be as small as possible. Therefore, the distribution will be more precise and that may reduce the number of subpopulations which leads to more accurate cdf. The study should also take a long time, thus all weather cases in the site will be taken in consideration.

Appendix A: Datasheet of the MPPT Charge Controller.

Table A.1: MPPT T40 main parameters.

Parameters / Model	MPPT10	MPPT20	MPPT30	MPPT40
Maximum power current	12A	20A	30A	40A
Installation Line (mm2）	4mm²	8mm²	10mm²	12mm²
Installation Line (AWG)	10(AWG)	8(AWG)	7(AWG)	6(AWG)
Weight	280g	300g	475g	480g
Dimensions	143×89×46（mm）		187*97*61（mm）	
System load loss	≤13mA			
Loop Buck	≤100mV			
Battery float voltage	13.8V（12V system）/27.6V（24V system）			
Battery (under voltage) protection	10.6V（12V system）/21.2V（24V system）			
Battery (undervoltage) recovery voltage	12.6V（12V system）/25.2V（24V system）			
Charge mode	MPPT+PWM MODE			
Operating Temperature	-10℃~60℃			
Storage Temperature	-30℃~70℃			
Humidity requirements	≤90％, No condensation			
Temperature compensation	-4mV/Cell/℃			

Appendix B: Datasheet of the Batteries.

Product Features

- Capacity range :26Ah —3000Ah.
- Voltage class:2V/6V/12V.
- Low self-discharge rate: ≤ 3%/month.
- Good high rate discharge performance.
- Long design life （ 25 5 years(≤28Ah).
- High sealed reaction efficiency: ≥ 99%.
- Wide operation temperature range: -20 ~60.
- Structure: compact design, shorter internal connectors between cells.
- Plate: Pasted flat type, with patent deep cycle formula of AM.
- Terminal: two or more types terminals are convenient for selection.
- Vent system: gases can be vented through flame arrester/ filter.
- Separator: using improved AGM separator, makes lower resistance; higher assembling pressure to increase deep cycle life.
- Battery case: made of high strength ABS(UL94-HB) and UL94-V0 is optional.
- Terminal sealing: double sealing technics (mechanical + epoxy gule).

Main Parameters

Table B.1: RITAR DC12-120 main parameters.

Model	Nominal Voltage	Capacity *C_{20}/C_5	Weight		Terminal Type	Dimension								Internal Resistance	Short Circuit Current	Terminal Position
						Length		Width		Height		Total Height				
	(V)	(Ah)	Lbs	Kg		mm	inch	mm	inch	mm	inch	mm	inch	(mΩ@25℃)	(A)	
DC12-26	12	26	17.86	8.1	F3/F13/T24	166	6.54	175	6.89	125	4.92	125	4.92	10.0	900	D
DC12-26S	12	26	18.30	8.3	F7/F11	165	6.50	126	4.96	174	6.85	174	6.85	11.5	850	D
DC12-28	12	28	18.96	8.6	F3/F13	166	6.54	175	6.89	125	4.92	125	4.92	9.0	950	D
DC12-28S	12	28	19.40	8.8	F7/F11	165	6.50	126	4.96	174	6.85	174	6.85	10.0	880	D
DC6-180	6	180	58.43	26.5	F12	306	12.05	168	6.61	222	8.74	227	8.94	3.0	3330	A
DC6-200	6	200	63.95	29	F16/F14	322	12.68	178	7.01	226	8.90	247	9.72	2.5	3700	A
DC6-200S	6	200	66.15	30	F12	260	10.24	180	7.09	247	9.72	252	9.92	2.5	3510	B
DC6-225S	6	225	70.56	32	F14	243	9.57	188	7.40	275	10.83	275	10.83	2.0	3980	B
DC12-40	12	40	28.67	13	F4/F11	198	7.80	166	6.54	171	6.73	171	6.73	8.0	1000	D
DC12-55	12	55	39.69	18	F15/F11	229	9.02	138	5.43	210	8.27	235	9.25	7.0	1100	C
DC12-65	12	65	46.31	21	F5/F11	350	13.78	167	6.57	180	7.09	183	7.20	6.5	1500	C
DC12-75	12	75	51.82	23.5	F15/F11	260	10.24	169	6.65	210	8.27	235	9.25	6.5	1720	C
DC12-75A	12	75	50.72	23	F15/F11	260	10.24	169	6.65	210	8.27	235	9.25	6.0	1720	C
DC12-80	12	80	52.92	24	F5/F11	350	13.78	167	6.57	180	7.09	183	7.20	6.0	1840	C
DC12-80A	12	80	50.05	22.7	F5/F11	350	13.78	167	6.57	180	7.09	183	7.20	6.5	1700	C
DC12-90	12	90	62.84	28.5	F15/F12	306	12.05	169	6.65	210	8.27	235	9.25	5.2	1940	C
DC12-90A	12	90	62.84	28.5	F15/F12	306	12.05	169	6.65	210	8.27	235	9.25	5.7	1850	C
DC12-100	12	100	66.15	30	F5/F12	328	12.91	172	6.77	222	8.74	222	8.74	5.0	2100	C
DC12-100A	12	100	63.95	29	F5/F12	328	12.91	172	6.77	222	8.74	222	8.74	5.0	2150	C
DC12-100S	12	100	63.95	29	F15/F12	306	12.05	169	6.65	210	8.27	235	9.25	4.8	2150	C
DC12-120	12	120	77.18	35	F5/F12	407	16.02	177	6.97	225	8.86	225	8.86	4.5	2220	C
DC12-120A	12	120	74.97	34	F5/F12	407	16.02	177	6.97	225	8.86	225	8.86	4.5	2220	C
DC12-120S	12	115	70.56	32	F5/F12	328	12.91	172	6.77	222	8.74	222	8.74	4.2	2130	C
DC12-134	12	134	91.51	41.5	F5/F12	340	13.39	173	6.81	280	11.02	285	11.22	4.5	2480	C
DC12-145	12	145	97.02	44	F5/F12	340	13.39	173	6.81	280	11.02	285	11.22	4.5	2630	C
DC12-150	12	150	98.12	44.5	F5/F12	483	19.02	170	6.69	240	9.45	240	9.45	4.2	2780	C
DC12-150A	12	150	96.36	43.7	F5/F12	483	19.02	170	6.69	240	9.45	240	9.45	4.5	2600	C
DC12-160	12	160	110.3	50	F16/F12	530	20.87	209	8.23	214	8.43	219	8.62	4.5	2960	E
DC12-180	12	180	116.9	53	F16/F12	530	20.87	209	8.23	214	8.43	219	8.62	4.0	3330	E
DC12-200	12	200	132.3	60	F16/F10	522	20.55	240	9.45	219	8.62	240	9.45	4.0	3700	E
DC12-200A	12	200	130.1	59	F16/F12	522	20.55	240	9.45	219	8.62	240	9.45	4.0	3430	E
DC12-225A	12	225	141.1	64	F16/F12	522	20.55	240	9.45	219	8.62	240	9.45	3.8	3980	E
DC12-260	12	260	163.2	74	F14	520	20.47	268	10.55	220	8.66	225	8.86	3.5	4810	E
FT12-55D	12	55	39.69	18	F11	291	11.46	106	4.17	222	8.74	230	9.06	6.0	1460	E
FT12-90D	12	90	58.43	26.5	F6/F11	563	22.17	114	4.49	188	7.40	188	7.40	5.8	2350	E
FT12-100D	12	100	66.15	30	F14/F8	508	20.00	111	4.37	236	9.26	236	9.29	5.2	2400	E
FT12-100AD	12	100	63.95	29	F14/F8	508	20.00	111	4.37	236	9.29	236	9.29	5.5	2400	E
FT12-100SD	12	110	68.36	31	F9	410	16.14	109	4.29	285	11.22	294	11.57	4.8	2850	E
FT12-105D	12	105	71.66	32.5	F14/F8	508	20.00	111	4.37	236	9.29	236	9.29	5.0	2400	E
FT12-110D	12	110	72.77	33	F9	410	16.14	109	4.29	285	11.22	294	11.57	4.8	2850	E
FT12-150D	12	150	95.92	43.5	F9	565	22.24	110	4.33	288	11.34	296	11.65	4.3	3250	E
FT12-160D	12	150	108.0	49	F9	565	22.24	110	4.33	288	11.34	296	11.65	4.2	3550	E
FT12-160AD	12	160	101.4	46	F9	565	22.24	110	4.33	288	11.34	296	11.65	4.2	3550	E
FT12-180D	12	180	114.7	52	F9	560	22.05	125	4.92	316	12.44	316	12.44	4.0	4150	E
FT12-185D	12	185	123.5	56	F9	560	22.05	125	4.92	316	12.44	316	12.44	4.0	4250	E
FT12-100LD	12	110	72.77	33	F9	394	15.15	109	4.29	285	11.22	285	11.22	4.8	2850	E
FT12-185LD	12	185	132.3	60	F9	560	22.05	125	4.92	316	12.44	316	12.44	4.0	4250	E

Appendix C: Datasheet of the Single -Phase Inverter.

Table C.1: Datasheet of Phoenix Inverter 24/800.

Phoenix Inverter 12 Volt / 24 Volt / 48 Volt	12/180 24/180	12/350 24/350 48/350	12/800 24/800 48/800	12/1200 24/1200 48/1200
Cont. AC power at 25°C (VA) (3)	180	350	800	1200
Cont. power at 25°C / 40°C (W)	175 / 150	300 / 250	700 / 650	1000 / 900
Peak power (W)	350	700	1600	2400
Output AC voltage / frequency (4)	110 VAC or 230 VAC +/- 3% 50 Hz or 60 Hz +/- 0,1%			
Input voltage range (V DC)	10,5 - 15,5 / 21,0 - 31,0 / 42,0 - 62,0		9,2 - 17,3 / 18,4 - 34,0 / 36,8 - 68,0	
Low battery alarm (V DC)	11,0 / 22 / 44		10,9 / 21,8 / 43,6	
Low battery shut down (V DC)	10,5 / 21 / 42		9,2 / 18,4 / 36,8	
Low battery auto recovery (V DC)	12,5 / 25 / 50		12,5 / 25 / 50	
Max. efficiency (%)	87 / 88	89 / 89/ 90	91 / 93 / 94	92 / 94 / 94
Zero load power (W)	2,6 / 3,8	3,1 / 5,0 / 6,0	6 / 5 / 4	6 / 5 / 6
Zero load power in search mode	n. a.	n. a.	2	2
Protection (2)	a - e			
Operating temperature range	-40 to +50°C (fan assisted cooling)			
Humidity (non-condensing)	max 95%			
ENCLOSURE				
Material & Colour	aluminium (blue Ral 5012)			
Battery-connection	1)	1)	1)	1)
Standard AC outlets	230V: IEC-320 (IEC-320 plug included), CEE 7/4 (Schuko) 120V: Nema 5-15R			
Other outlets (at request)	BS 1363 (United Kingdom) AN/NZS 3112 (Australia, New Zealand)			
Protection category	IP 20			
Weight (kg / lbs)	2,7 / 5,4	3,5 / 7,7	6,5 / 14.3	8,5 / 18.7
Dimensions (hxwxd in mm) (hxwxd in inches)	72x132x200 2.8x5.2x7.9	72x155x237 2.8x6.1x9.3	104 x 194 x 305 4.1 x 7.6 x 12.0	104 x 194 x 305 4.1 x 7.6 x 12.0
ACCESSORIES				
Remote on-off switch	Two pole connector			
Automatic transfer switch	Filax			
STANDARDS				
Safety	EN 60335-1			
Emission Immunity	EN 55014-1 / EN 55014-2/ EN 61000-6-2 / EN 61000-6-3			

1) Battery cables of 1.5 meter (12/180 with cigarette plug)
2) Protection key:
a) output short circuit
b) overload
c) battery voltage too high
d) battery voltage too low
e) temperature too high
3) Non-linear load, crest factor 3:1
4) Frequency can be set by DIP switch (48/350 model only)

References

[1]: Article “History of Solar cell” US Department of Energy Efficiency and Renewable Energy. https://www1.eere.energy.gov/solar/pdfs/solar_timeline.pdf, 04-13-2019.

[2]: Fundamental Properties of Solar Cells, Principles and Varieties of Solar Energy. The University of Toledo, Department of Physics and Astronomy SSARE, PVIC.January 10, 2012.

[3]: Afshin Izadian, Arash Pourtaherian, and Sarasadat Motahari., “Basic Model and Governing Equation of Solar Cells used in Power and Control Applications”, Published in: 2012, IEEE Energy Conversion Congress and Exposition (ECCE).

[4]: Wilhelm Durisch, Dierk Tille, A. Wörz and Waltraud Plapp.” Characterisation of photovoltaic generators”, published by Elsevier in April 2000.

[5] G. Cook, L. Billman, and R. Adcock, “Photovoltaic Fundamental”, DOE/Solar Energy Research Institute Report No. DE91015001, 1995.

[6] https://www.pveducation.org. 05-18-2019.

[7] Gilbert M. Masters, Renewable and Efficient Electric Power Systems, A JOHN WILEY & SONS, INC., PUBLICATION, 2004.

[8] Indra Bahadur Karki, “Effect of Temperature on the I-V Characteristics of a Polycrystalline Solar Cell”, Journal of Nepal Physical Society, August-2015, Vol. 3, No. 1

[9] Manual Life Data Analysis Reference, http://www.ReliaSoft.com. 05-06-2019.

[10] Diane L. Evans1, John H. Drew2, and Lawrence M. Leemis2,” The Distribution of the Kolmogorov–Smirnov, Cramer–von Mises, and Anderson–Darling Test Statistics for Exponential Populations with Estimated Parameters”, Communications in Statistics Simulation and Computation, 2008.

[11] https://www.altestore.com/store/info/solar-charge-controller/. 05-17-2019.

[12] “solar system charge controllers”, ECE Tutorials Electronics and control Systems, http://ecetutorials.com/power-plant/solar-system-charge-controllers/. 05-17-2019.

[13] M. LAMNADI, M. TRIHI, Badre BOSSOUFI, A. BOULEZHAR, “COMPARATIVE STUDY OF IC, P&O AND FLC METHOD OF MPPT ALGORITHM FOR GRID CONNECTED PV MODULE”, Morocco university.

[14] R. Faranda and S. Leva, “Energy comparison of MPPT techniques for PV Systems”, WSEAS Transactions on Power Systems, vol. 3,2008, pp. 448.

[15] Muhammad H. Rashid – “Power electronics handbook_ Devices”, circuits and Applications-Academic Press, 2006.

[16] Guda, H. A. and Aliyu U. O,” Design of a Stand-Alone Photovoltaic System for a Residence in Bauchi”, Department of Electrical and Electronics Engineering Abubakar Tafawa Balewa University, PMB 0248, Bauchi, Nigeria.

[17] Leonard J. Kazmier,” SCHUM’S outlines PROBABIBILITY, RANDOM VARIABALES, & RANDOM PROCESS”, fourth edition, NO: 0-07-141080-5.